Accepted Manuscript

Geological Society, London, Memoirs

The Seismic Structure of the Antarctic Upper Mantle

Douglas A. Wiens, Weisen Shen & Andrew Lloyd

DOI: https://doi.org/10.1144/M56-2020-18

To access the most recent version of this article, please click the DOI URL in the line above. When citing this article please include the above DOI.

Received 30 June 2020 Revised 29 March 2021 Accepted 31 March 2021

© 2021 The Author(s). This is an Open Access article distributed under the terms of the Creative Commons Attribution 4.0 License (http://creativecommons.org/licenses/by/4.0/). Published by The Geological Society of London. Publishing disclaimer: www.geolsoc.org.uk/pub ethics

Manuscript version: Accepted Manuscript

This is a PDF of an unedited manuscript that has been accepted for publication. The manuscript will undergo copyediting, typesetting and correction before it is published in its final form. Please note that during the production process errors may be discovered which could affect the content, and all legal disclaimers that apply to the book series pertain.

Although reasonable efforts have been made to obtain all necessary permissions from third parties to include their copyrighted content within this article, their full citation and copyright line may not be present in this Accepted Manuscript version. Before using any content from this article, please refer to the Version of Record once published for full citation and copyright details, as permissions may be required.

The Seismic Structure of the Antarctic Upper Mantle

Douglas A. Wiens^{1*}, Weisen Shen² & Andrew Lloyd³

¹Department of Earth & Planetary Sciences, Washington University in St. Louis, St. Louis, MO 63130, USA

² Department of Geosciences, Stony Brook University, Stony Brook, NY, USA

³Lamont-Doherty Earth Observatory, Columbia University, Palisades, NY, USA

ORID: DW, 0000-0002-5169-4386

*Correspondence: doug@wustl.edu

Abstract:

The deployment of seismic stations and the development of ambient noise tomography and new analysis methods provide an opportunity for higher resolution imaging of Antarctica. Here we review recent seismic structure models and describe their implications for the dynamics and history of the Antarctic upper mantle. Results show that most of East Antarctica is underlain by continental lithosphere to depths of ~ 200 km. The thickest lithosphere is found in a band 500-1000 km west of the Transantarctic Mountains, representing the continuation of cratonic lithosphere with Australian affinity beneath the ice. Dronning Maud Land and the Lambert Graben show much thinner lithosphere, consistent with Phanerozoic lithospheric disruption. The Transantarctic Mountains mark a sharp boundary between cratonic lithosphere and the warmer upper mantle of West Antarctica. In the Southern Transantarctic Mountains, cratonic lithosphere has been replaced by warm asthenosphere,

giving rise to Cenozoic volcanism and an elevated mountainous region. The Marie Byrd Land volcanic dome is underlain by slow seismic velocities extending through the transition zone, consistent with a mantle plume. Slow velocity anomalies beneath the coast from the Amundsen Sea Embayment to the Antarctic Peninsula likely result from upwelling of warm asthenosphere during subduction of the Antarctic-Phoenix spreading center.



Introduction

Seismological imaging provides essential constraints on the physical processes and conditions shaping the upper mantle beneath Antarctica. Unlike other continents, the Antarctic mantle is overlain not only by the crust and sedimentary cover, but also by a thick ice sheet, greatly limiting geological mapping and sampling. Thus, seismological studies applied to Antarctica fulfil a unique role, by providing information on poorly constrained geological processes that have formed the continent. The ice sheets also constitute large, temporally varying loads which cause deformation of the mantle and the land surface through glacial isostatic adjustment. Seismology is able to characterize lateral variations in the temperature profile of the upper mantle and crust and thus constrain the geothermal heat flux (Shapiro and Ritzwoller, 2004; Shen et al, 2020). These thermal properties control the response of the mantle and the land surface to glaciation (Ivins and Sammis, 1995; Ivins and James, 2005; van der Wal et al., 2015; Ivins et al, this volume), and affect the future evolution of the ice sheet (Gomez et al, 2015; Whitehouse et al. 2019).

Seismographs were part of the scientific agenda for Antarctic exploration from the very first expeditions. A Milne seismograph was operated by Robert F. Scott's Discovery Expedition (1901-1904) for more than a year at Hut Point, near modern-day McMurdo Station, and dozens of earthquakes were detected (Bernacchi and Milne, 1908). A seismograph was installed at the South Pole base during the International Geophysical Year in 1957. However, despite these early efforts, it was not until the turn of the century that autonomous seismographs were installed in Antarctica, allowing the underlying structure of the continent to be revealed at greater resolution.

The last two decades have seen rapid progress in both seismological instrumentation in Antarctica and in seismic analysis methods to utilize these data. The results of these efforts are detailed seismological models describing the three-dimensional structure of the Antarctic upper mantle, as well as crustal thickness. Here we review these models and briefly describe their implications for understanding the dynamics and history of the Antarctic upper mantle. This review concentrates on large-scale studies of upper mantle structure from analysis of passive seismic recording, while recognizing that active source seismic studies provide important details in some specific regions.

Seismic Data and Analysis Methods

Antarctic Seismic Data

From the 1950s through the 1990s, seismographs were largely restricted to a few permanently occupied bases. With the exception of South Pole, these were generally along the coasts, so the interior of Antarctica was relatively unexplored from a seismological standpoint. Thus, maps of Antarctic mantle structure from that time period showed very limited resolution compared to other parts of the world. Active source seismic refraction lines did provide estimates of crustal thickness and uppermost mantle P-wave velocity in several places (Bentley et al., 1973; Ten Brink et al., 1993; Leitchenkov and Kudryavtzev, 1997; Trey et al, 1999).

The advent of technology for operating autonomous broadband seismographs in remote parts of the Antarctic interior has revolutionized seismic studies in Antarctica over the past two decades. Initial projects, including SEPA (Robertson-Maurice et al., 2003), ANUBIS (Anandakrishnan et al., 2000), TAMSEIS (Lawrence et al., 2006), SSCUA (Reading, 2006), and a deployment in the Transantarctic Mountains (Bannister et al., 2003) generally operated stations only in the summer months. However, more recent large-scale deployments such as AGAP/GAMSEIS (Hansen et al., 2010), Ross Ice Shelf (Baker et al., 2019), TAMNNET (Hansen et al., 2015), and UKANET

(O'Donnell et al., 2019) have provided high quality data year-round. In many cases the seismographs remained deployed for only about two years, though the POLENET/A-NET project (Accardo et al., 2014) has maintained some remote autonomous stations for over a decade. Fig. 1 shows the distribution of Antarctic broadband seismic stations providing data for analyses discussed here. The combined distribution of seismic stations provides reasonably good coverage at the several hundred km level in West Antarctica, but vast regions of East Antarctica remain without instrumentation.

Body wave tomography and receiver functions

P and S-wave tomography using teleseismic arrivals can provide strong constraints on lateral velocity variations in the upper mantle of Antarctica (Watson et al., 2006; Lloyd et al., 2013; 2015; Hansen et al., 2014; Brenn et al., 2017; White-Gaynor et al., 2019; Lucas et al., 2020). In these studies, arrival time anomalies across a seismic array are calculated from P or S waveforms using cross correlation, and the travel time anomalies are then inverted for the velocity structure beneath the array. These studies typically yield detailed images of lateral velocity variations, but provide limited constraints on the depths of the velocity anomalies. Continent-wide body wave tomography models suffer from highly variable resolution, with good resolution in areas with greater seismic station density such as parts of West Antarctica, and poor resolution in regions of sparse station coverage.

Body wave arrivals can also be analyzed for structural interfaces or discontinuities below the seismic station using receiver function methodology. This method processes the horizontal and vertical components of body waves to enhance arrivals converted from *S* to *P* or *P* to *S* at structural interfaces (e.g. Ammon et al, 1991). In general, P-wave receiver functions yield good resolution of Moho depth as well as shallow interfaces, and have provided estimates of crustal thickness for many locations around the continent (Bannister et al., 2003; Reading, 2006; Chaput et al., 2014; Ramirez et al., 2017). For some areas with a thick ice sheet, S-wave receiver functions provide better results because the Moho conversion is not obscured by reverberations of seismic energy in the ice (Hansen et al, 2009; 2010; Ramirez et al., 2016). P-wave receiver functions are also used to study the depth of the 410 and 660 km discontinuities in the mantle and thus infer the thickness of the transition zone (Reusch et al. 2008; Emry et al., 2015; 2020). The thickness of the transition zone allows identification of temperature anomalies at transition zone depths, due to the different signs of the Clapyron slopes of the olivine to wadsleyite and ringwoodite to bridgemanite phase transitions denoted by these discontinuities (e.g. Bina and Helffrich, 1994).

Surface waves from earthquakes and ambient noise

Surface wave tomography can image the crust and upper mantle with superior depth resolution, due to the relationship between surface wave dispersion and velocity structure with depth. However, good resolution is generally limited to the upper 200-250 km of the earth, and the resulting structures are usually quite smooth, without sharp interfaces. Traditional surface wave methods involve analyzing individual seismograms to determine the surface wave group and phase velocity along the path from earthquake to receiver, and then performing a tomographic inversion at each period to generate phase and group velocity maps (Roult et al., 1994; Danesi and Morelli, 2001; Ritzwoller et al, 2001). These maps can then be inverted to determine shear velocity at each location. The inclusion of higher mode Rayleigh wave measurements improves the resolution at depths greater than 200 km (Sieminski et al., 2003). In some cases, the surface wave group velocity measurements may be inverted directly for shear velocity (An et al., 2015).

Denser arrays of seismographs on the Antarctic interior can be used to determine the phase velocity of Rayleigh waves from teleseismic earthquakes traveling across the continent (Lawrence et al., 2006). In one implementation, the incoming Rayleigh waves are approximated as two interfering plane waves, with seismograms then analyzed to determine phase velocity images as a function of period, which are then inverted for velocity structure (Forsyth and Li, 2005; Heeszel et al., 2013; 2016). Surface wave phase and group velocities can also be measured from seismic Green's functions derived by cross correlating ambient noise at station pairs. This approach produces more accurate results than measurements from earthquake records at short periods (Shapiro et al., 2005; Pyle et al., 2010). Phase velocities determined by ambient noise at shorter periods (~ 8-45 s) are often combined with phase velocities from earthquakes at longer periods (~ 25-120 s) to provide phase velocities across a wide period band and constrain both shallow crustal and deeper mantle structure (Shen et al, 2018; O'Donnell et al., 2019a). In areas with thinner crust such as the Ross Embayment, the addition of ambient noise provides key constraints to the uppermost mantle structure.

Seismic anisotropy analysis

Seismic anisotropy, or the directional dependence of seismic velocities resulting from directional dependence of the elastic moduli, has the potential to reveal further information about mantle structure and processes. Seismic anisotropy is often a result of lattice preferred orientation, which is the alignment of the crystallographic axes of anisotropic minerals by rock fabric or deformation. Alternatively, seismic anisotropy can result from shape preferred orientation, or the alignment of geometric objects of different seismic velocity, such as elongated minerals, or larger objects such as dikes or sills. Studies of naturally deformed mantle xenoliths (Mainprice and Silver 1993; Chatzaras and Kruckenberg, this volume), as well as laboratory studies of artificially deformed olivine aggregates (Zhang and Karato, 1995) indicate that mantle seismic anisotropy generally results from lattice preferred orientation. The fast axis of anisotropy is usually parallel to the extension direction, or to the flow direction if there is a flow fabric, although other orientations are possible under conditions of high water or high stress (Karato et al, 2008). Thus, mantle anisotropy is commonly used to indicate the extension direction of mantle deformation or the direction of mantle flow.

Seismic observations cannot fully determine the general elastic tensor for anisotropic media, so several different techniques are used to constrain different aspects of anisotropy. Radial anisotropy (transverse isotropy), can be thought of as the difference between vertical (V_{SV}) and horizontally (V_{SH}) polarized shear wave velocities, and is usually measured by jointly analyzing Love and Rayleigh surface waves. The uppermost mantle shows positive radial anisotropy ($V_{SH} > V_{SV}$) in most places worldwide (Panning and Romanowicz, 2006; Kustowski et al, 2008). Seismic models for Antarctica also show strong positive radial anisotropy (Ritzwoller et al, 2001; Lloyd, 2018; Zhou et al., 2019; ODonnell et al., 2019b), although the spatial pattern is not well resolved.

Azimuthal anisotropy can be evaluated by measuring the variation of P, S, or surface wave velocities with azimuth, or by shear wave splitting measurements. Shear waves propagating through an anisotropic media are split along fast and slow vibration planes, allowing the fast direction and magnitude of anisotropy to be estimated. SKS and SKKS phases from distant earthquakes are particularly useful, since they eliminate the possibility that the anisotropy is near the source, and results are commonly interpreted as upper mantle anisotropy beneath the receiver (Silver, 1996; Savage, 1999). Several SKS splitting studies have been carried out in Antarctica (Muller 2001; Bayer *et al.* 2007; Reading & Heintz 2008; Barklage *et al.* 2009; Accardo et al., 2014). Results show strong azimuthal anisotropy in parts of West Antarctica (Fig. 2), and indicate that the average upper

mantle azimuthal anisotropy of West Antarctica is greater than that of East Antarctica (Accardo et al. 2014; Lucas et al., unpublished results). The anisotropy fast directions show a complex pattern related to the tectonic development of the region. The directions do not generally align with the velocity of the Antarctic Plate in an absolute reference frame, indicating that the anisotropy is not due to mantle shear from the continent moving relative to the deeper mantle (Accardo et al., 2014).

Bayesian joint inversion

The large-scale collection of broadband seismic data at regional or continental scales over the past two decades has enabled the joint analysis of multiple types of seismic observations. Local surface wave dispersion properties and P-wave Moho conversion waveforms (i.e., receiver functions) are typical choices since they can be incorporated into a relatively simple local inversion for a 1-dimensional (1-D) model (Julia et al., 2000; Lawrence and Wiens, 2004; Chang et al., 2004). Among various realizations, the joint inversion under the Bayesian framework has been popular, since the associated uncertainties of the resulting 3-dimensional model can be quantified from the Monte Carlo sampling.

For Antarctica, this approach has been applied to data collected by more than 200 seismic stations deployed between 1998 and 2017. Shen et al., (2018b) constructed a new seismic model for central and West Antarctica by jointly inverting Rayleigh wave phase and group velocities along with P-wave receiver functions. In this work, ambient noise tomography is used to construct Rayleigh wave phase and group velocity dispersion maps at relatively short periods (8 to 40 sec), and teleseismic earthquakes derived phase velocity maps at longer periods (32 to ~ 140 sec) are taken from Heeszel et al. (2016). Comparison between the two sets of phase velocity maps at 30 sec presents a difference of -0.002+/-0.027 km/sec (< 0.1% on average) for phase velocity in West and central Antarctica. This difference level is similar to the analogous comparison made in N. America where seismic stations were denser, showing that high quality ambient noise tomography can be applied to the remote continent.

These Rayleigh wave phase and group velocity maps, together with P receiver function waveforms, were then used to construct a new 3-dimensional (3-D) shear velocity model for the crust and uppermost mantle using a Bayesian Monte Carlo algorithm. Since the velocities are determined from Rayleigh waves, the maps show the velocity of vertically polarized shear waves (V_{SV}). Each Bayesian Monte Carlo inversion provides an ensemble of 1-D models that fit both types of data. A final 3-D model is then constructed by taking the average 1-D models from the ensembles, and associated uncertainties are defined by the standard deviation of the ensembles. An example of the inversion procedure for a station in East Antarctica is shown in Fig 3., giving the fit of the preferred model to the surface wave data (3a) and P-wave receiver function (3b). Incorporation of the P-wave receiver function into the inversion reduces the uncertainty in the Moho depth and crustal velocities, as shown by the comparison of the resulting structure and standard deviation (Fig 3 c-d) and prior and posterior distributions (Fig 3 f-h) for the joint inversion as well as the inversion of surface wave data alone. A similar Monte Carlo approach applied to Rayleigh and Love wave dispersions has helped construct a 3-D anisotropic model for the crust (Zhou et al., 2019).

The resulting 3-D seismic model covers most of West Antarctica and parts of East Antarctica where there is adequate seismic station coverage for this method (Fig. 4), and extends down to the limit of good depth resolution with fundamental mode Rayleigh waves (about 200 km). The shear velocity maps show a clear dichotomy of the tectonically active West Antarctica and the stable and

ancient (Fig. 4). In addition, the model shows significant velocity anomalies within both West Antarctica and the central part of East Antarctica, which will be discussed later in this paper.

Adjoint tomography

The use of 3-D numerical wavefield simulations (Komatitsch and Villote, 1998; Komatitsch and Tromp, 1999) along with adjoint inversion methods (e.g., Tarantola, 1984; Tromp et al., 2005) are proving to be a powerful tool for imaging Earth's seismological structure (e.g., Fitchner et al., 2009; Tape et al., 2010; Zhu et al., 2015; Bozdağ et al., 2016). Although computationally expensive, these iterative methods are advantageous because they account for many of the complexities associated with seismic wave propagation in a complex 3-D medium, and thus allow for the accurate and efficient determination of synthetic seismograms and sensitivity kernels for all body and surface wave arrivals (Komatitsch & Tromp, 2002a, 2002b). The ability to use a much larger portion of the seismic wavefield in comparison to traditional seismic imaging, to accurately map out the observational sensitivities to Earth structure, and to avoid simplifying assumptions such as the high frequency approximation of ray theory, permits higher fidelity seismic images over large and poorly sampled regions.

Lloyd et al. (2020) used this iterative adjoint tomographic inversion to seismically image the entire Antarctic continent and the surrounding southern oceans to depths of 800 km at resolutions approaching that of regional studies. The resulting radial anisotropic model (ANT-20; Fig. 6) was determined following 20 iterations, with a 3-D starting model based on the global mantle model S362ANI (Kustowski et al., 2008) and a modified version of CRUST1.0 (see Lloyd et al., 2020). During each iteration, the model was updated to include increasingly shorter wavelength features based on travel time observations between observed and synthetic earthquake seismograms. These observations include P, S, Rayleigh, and Love waves, including reflections and overtones, from 270 earthquakes recorded at 323 seismic stations, many of which are shown in Fig. 1. Since ANT-20 uses both Love and Rayleigh waves to produce a radially anisotropic model, maps of velocity heterogeneity show the Voigt average shear velocity:

$$V_{S_voigt} = \frac{\sqrt{V_{sh}^2 + 2V_{sv}^2}}{3} \tag{1}$$

Because V_{SH} is generally faster than V_{SV} in the upper mantle, the Voigt average velocities are about 1-2% faster than V_{SV} .

The high computational cost of the adjoint inversion, ~3 million CPU hours to produce ANT-20, limits the ability to assess the model's resolution or uncertainty. Thus, evaluation of resolution relies on proxies for data density and point-spread function tests. These tests show that structure appearing in ANT-20, south of 60 degrees S, is reliably resolved within the upper mantle and transition zone (Lloyd et al., 2020). The length scales of the imaged features are limited by the smoothing employed in the inversion. The lateral smoothing length ranges from ~140 km in the upper mantle to ~340 km in the transition zone, while the vertical smoothing length is held fixed at ~45 km at all depths throughout the inversion. These facts, combined with comparisons to regional seismic models (e.g., Heeszel et al., 2016; Shen et al., 2018; O'Donnell et al., 2019) and other geophysical observations indicate ANT-20 possesses similarly high resolution, but across the entire Antarctic region.

East Antarctica

Antarctica is divided into two very different geological subcontinents, with East Antarctica (EA) representing largely Precambrian cratonic units and West Antarctica (WA) consisting of terranes formed or tectonically modified during the Mesozoic and Cenozoic. Most of EA shows crustal thicknesses that are typical for continental cratons (Pappa et al., 2019b; Szwillus et al., 2019), whereas WA shows thinner crust similar to crustal thicknesses found in regions of extended Phanerozoic continental crust (Fig 5). Although Archean to early Paleozoic outcrops have been sampled and mapped near the coasts and in the Transantarctic Mountains (Tingey, 1991; Fitzsimons, 2000; Goodge et al, 2001), most of the EA interior is covered by thick ice sheets, greatly limiting our understanding of its geology. Thus, seismology and other geophysical techniques play an outsized role in constraining the formation and geological history of EA.

Most of EA is underlain by thick continental lithosphere, as defined by strong positive velocity anomalies relative to global averages, that extends to depths of greater than 200 km in several places (Figs 6-7). Similar to mantle lithosphere beneath other cratons worldwide, this continental lithosphere represents ancient, cooled mantle that that may be isopycnic and thus stable due to competing thermal and compositional buoyancy forces (Jordan, 1981; Sleep, 2005). The fast shear velocities arise predominantly from cold temperatures due to conductive cooling and to a lesser extent from a depleted mantle chemistry (e.g., Lee, 2003; Schutt and Lesher, 2006). For other continental cratons with extensive xenolith data, there is good agreement between mantle temperature profiles inferred from mantle xenoliths and shear velocities, with both indicating thick, cold lithosphere extending to depths of greater than 200 km (Priestley and McKenzie, 2006).

Although most of EA shows seismic velocity anomalies of about 5-6% fast at depths of 75-150 km, greater variability in seismic velocity is found beneath the East Antarctic Highlands, stretching from western Dronning Maud Land to the Lambert Graben, containing several regions with mantle velocities close to the global average (Fig. 6). This contrasts with several regions in central Antarctica show fast velocity anomalies as large as 7-8% and lithospheric thicknesses of greater than 200 km. The variation in mantle lithospheric thickness and seismic velocity profiles allows us to better understand the distribution of lithospheric terrane ages within EA and place constraints on the geological evolution of the continent.

The fastest seismic velocities and the thickest continental lithosphere, extending to depths of greater than 200 km, occur along a band extending almost entirely across Antarctica 500-1000 km inboard from the Transantarctic Mountains (Fig. 7). Some of the thickest lithosphere is found inboard of the Miller Range in the Transantarctic Mountains where 3.15 to 3.05 Ga Nimrod Complex rocks confirm the existence of Archean-age terranes, although Mesoproterozoic units are also found that region (Goodge and Fanning, 1999; 2016), and glacial granitoid clasts show ages ranging from 2.01 to 1.06 Ga (Goodge et al., 2017). The thick lithosphere extends to the Shackleton Range, near the Weddell Embayment, where Paleoproterozoic rocks are preserved (Brommer et al., 1999; Will et al., 2009). Boger (2011) proposed that the "Shackleton" and "Nimrod" cratons are connected to late Archean "Gawler Craton" rocks exposed in Australia (Swain et al., 2005) and along the corresponding Tierra Adélie coast of Antarctica (Oliver and Fanning, 2002). The continuity of magnetic anomalies between the Antarctic and Australian coasts provides further evidence for the continuity of these cratonic regions prior to Gondwana breakup (Pappa and Ebbing, this volume). The resulting "Mawson Continent" extends entirely across EA from the coast on the Australian side to just southeast of the Weddell Embayment. The distribution of the fastest seismic velocities and

thickest lithosphere in the Lloyd et al. (2020) seismic velocity structure correlates well with the proposed extent of the Mawson Continent, supporting the idea that this region represents the late Archean to Paleoproterozoic cratonic nucleus of Gondwana.

Thick, cold lithosphere also extends beneath the Gamburtsev Subglacial Mountains, an enigmatic highland in central Antarctica with peaks reaching to 3000 m (Ferraccioli et al., 2011).

Surface wave (Heeszel et al., 2013) and body wave (Lloyd et al, 2013) tomography show that lateral variation in mantle velocity is modest, precluding significant Mesozoic or Cenozoic mantle tectonism or rejuvenation. A systematic comparison of Rayleigh wave phase velocity curves worldwide shows that the Gamburtsev Mountains phase velocities are best matched by Archean and Paleoproterozoic regions, suggesting the mountains are underlain by ancient continental lithosphere (Heeszel et al., 2013). Shen et al (2018) found that uppermost mantle velocities (Moho to 100 km depth) below the Gamburtsev Mountains are anomalously low, by 2-4%, relative to expected lithospheric craton velocities. They are also lower than surrounding regions of EA and the deeper lithosphere. A detailed discussion in Shen et al. (2018) demonstrated that this anomaly is unlikely to have a thermal origin, but is most likely the signature of a compositionally anomalous body, perhaps remnant from a continental collision in Proterozoic or early Paleozoic time (Ferraccioli et al, 2011; An et al., 2015).

The mountain elevations are largely supported by crustal thicknesses of up to about 55 km (Hansen et al., 2010; see Fig. 5). Initial crustal thickening likely occurred through a compressional orogeny in the Neoproterozoic to earliest Paleozoic, consistent with detrital zircon studies (van de Flierdt et al., 2008), with additional uplift associated with the extension of the Lambert Graben in the late Paleozoic to early Mesozoic associated with the early stages of Gondwana breakup (Phillips and Laufer, 2009; Maritati et al., 2020), and preservation of topography due to low erosion rates (Heeszel et al., 2013; Lloyd et al., 2013).

Much greater variability in lithospheric thickness is found beneath the highlands stretching from western Dronning Maud Land to the Lambert Graben (Figs 6-7). Thinner lithosphere, with thicknesses on the order of 100 km, is found throughout much of this region. The uppermost mantle beneath a portion of Dronning Maud Land is characterized by an absence of fast lithosphere, despite rock ages that extend from Mesoproterozoic to Early Paleozoic. The absence of lithosphere in a region of Paleozoic or earlier age suggests that the lithosphere has been tectonically destabilized or removed at a later time. The absence of fast shear velocities at depths of 70-150 km suggests that the Precambrian age lithosphere of this region has been removed, most likely by delamination (Lloyd et al, 2020). Unlike regions of Cenozoic delamination, which are characterized by low upper mantle velocities as hot asthenosphere has replaced lithosphere (e.g. Levander et al., 2011; Shen et al., 2018a), uppermost mantle velocities in this region are near the global average. Thus, the asthenosphere that replaced the foundered lithosphere has already cooled, indicating a delamination event that occurred prior to the Cenozoic. Jacobs et al. [2008] suggested a delamination event occurring at ~500 Ma to explain the late-tectonic granitoid intrusions found in Dronning Maud Land, consistent with the seismic structure.

The Lambert Graben and other neighboring regions to the west represents an ancient terrane, with basement rocks ranging from Archean to earliest Paleozoic (Fitzsimons, 2000), that also lacks thick continental lithosphere (Figs 6-7). Seismic structures in this region show that high lithospheric velocities are limited to depths shallower than 75-100 km, suggesting the existence of thin lithosphere, in contrast to surrounding regions where high velocities extend to \sim 200 km (Lloyd et al, 2019). The Lambert Graben and corresponding rift structures in India developed during

Carboniferous to early Cretaceous extension associated with the breakup of Gondwana (Phillips and Laufer, 2009). Xenolith suites from the Lambert Graben indicate a transition from a relatively cold to a warmer geotherm, likely during the late Paleozoic early rifting stages and Mesozoic formation of the graben (Foley et al., 2006; Foley et al., this volume). Thus, mantle geodynamic processes associated with this extension and rifting likely heated and destabilized the existing Precambrian lithosphere, thinning or removing it.

Transantarctic Mountains and Adjacent Rifts

The Transantarctic Mountains (TAMS) are traditionally viewed as the tectonic boundary between the thick Precambrian cratonic lithosphere of EA and the Phanerozoic lithosphere domains of WA, although there is some evidence that crust of EA affinity extends to the middle of the Ross Sea (Tinto et al., 2019). The 4,000 km-long mountain range with peaks of up to ~ 4,000 m exhibits strong along-strike variations, varying from a narrow, rift-shoulder-like orogeny in the central TAMS to the 400-km broad, plateau-like elevated areas in the southernmost and northernmost segments. These variations in topography reflect a complicated history of tectonism along the TAMS, and correlate with changes in the underlying upper mantle structure, as imaged in the latest seismic models (Shen et al., 2018; Lloyd et al. 2020).

Seismic tomography reveals a band of slow velocities extending from the Macquarie Triple Junction, through the volcanic Balleny Islands, the extinct Adare Trough spreading center, and along the front of the TAMS (Fig 6). This pattern suggests that the Transantarctic Mountains and Terror Rift are part of a larger tectonic system linked to mantle geodynamic processes, stretching from the mid-ocean ridge to the Southern TAMS. The Adare Trough, located just north of the Ross Embayment near the northern terminus of the Transantarctic Mountains, displays magnetic anomalies resulting from sea floor spreading from 46 to 26 Ma (Granot et al., 2013), with slow spreading continuing to 11 Ma and evidence of extensional faulting up to the present (Granot & Dyment, 2018). The western side of the Ross Embayment accommodated almost 100 km of extension from 40 -26 Ma associated with plate motion between East and West Antarctica (Wilson and Luyendyk, 2009; Granot et al., 2013; Davey et al., 2016). Very slow extension and rift sedimentation occurred since that time along the Terror Rift, which parallels the TAMS along the western Ross Embayment (Fielding et al., 2008; Martin and Cooper, 2010; Granot and Dyment, 2018). The slow wave speeds show that the upper mantle retains warm uppermost mantle temperatures caused by an extensional tectonic environment despite the fact that tectonic motion along this boundary has largely ceased, as shown by the absence of resolvable motion in GPS surveys (T. Wilson, pers. comm). Anomalously warm upper mantle temperatures are also indicated for this region by mantle xenolith studies (e.g. Martin et al., this volume).

The northern section of the Transantarctic Mountains mostly constitutes the highlands of Northern Victoria Land (NVL). Surface and body wave tomography using a regional temporary seismic array revealed that a slow velocity anomaly in the upper mantle between Moho and 150 km depth is located near the coastline of NVL (Hansen et al., 2015; Graw et al, 2016; Brenn et al., 2017). The continental scale model from Lloyd et al., (2020) shows a large slow velocity region in the uppermost mantle beneath the high elevations of northernmost Victoria Land and the adjacent areas of the Ross Embayment that connect the Balleny Islands to the north and Ross Island to the south (Fig 6). This extended region of low velocity in the upper mantle implies a strong thermal contribution to the uplift of NVL.

Detailed body and surface wave tomography using temporary seismic stations shows a sharp boundary between slow and fast upper mantle, near the crest of the TAMS near Ross Island (Lawrence et al., 2006a; Watson et al., 2006; Brenn et al., 2017; Shen et al., 2018; White-Gaynor et al., 2019). There is also a sharp boundary along the TAMS between low mantle seismic attenuation in EA and high mantle attenuation beneath Ross Island and the Terror Rift (Lawrence et al., 2006b). The slow wave speeds in this region are consistent with the general absence of lithosphere and high upper mantle temperatures expected beneath a recently extending rift zone with a small amount of continuing decompression melting.

Active volcanism along the western coast of the Ross Embayment, mostly over the past 10 Ma, extends from the northernmost tip of the coastline to just south of Ross Island (Kyle, 1990). A mantle plume origin has been proposed for Mt Erebus, on Ross Island, based largely on petrological and geochemical data (Kyle, 1992; Phillips et al., 2018), although other studies associate the volcanism with mantle metasomatism from the long subduction history in this region (Day et al., 2019; Martin and Smellie, 2020). Adjoint tomography shows that Ross Island is underlain by a prominent slow velocity anomaly extending down to the 410 km discontinuity, but anomalies beneath this are low amplitude and indistinct (Lloyd et al., 2020). P-wave travel-time tomography also shows prominent upper mantle slow velocity anomalies, but the anomalies diverge laterally in the transition zone (Hansen et al., 2014; White-Gaynor et al., 2019). This does not necessarily eliminate the plume model, since geodynamical modeling suggests that plumes may be highly tilted in the mid mantle (Bredow and Steinberger, this volume). Emry et al (2020), using receiver functions, found that the mantle transition zone was anomalously thin near Mt Erebus and along the adjacent TAMS, suggesting a warm thermal anomaly in the transition zone. French and Romanowicz (2015), a global tomographic study, shows little anomaly in the transition zone, a significant slow anomaly at depths of 800-1200 km, and no anomalies in the lower mantle (Phillips et al., 2018). Thus, it is clear that the region is underlain by a significant thermal anomaly in the upper mantle, but the existence of a classic mantle plume arising near the core-mantle boundary remains uncertain.

The southern section of the TAMS shows some unusual characteristics compared with other sections of the TAM. First, unlike the nearby central Transantarctic Mountains where the exposed high mountains are only ~ 100 km wide, the Southern TAMS has a plateau-like elevated region extending into EA for ~ 400 km. Secondly, unlike the central and northern TAMS where volcanic rocks are usually found on the West Antarctic Rift (WARS) side of the high mountains, volcanism of Sheridan Bluff and vesicular basalts of the Mount Early (Fig. 2) that exhibit Miocene age (~ 15-20 Ma) are all located on the EA side of the peaks (Stump et al., 1980). Notably, recently found volcanic rocks in glacial deposits show ages of 25-17 Ma and can be traced to the magnetic anomaly 400 km into EA (Licht et al., 2018, Fig. 2). Both the topographic and volcanic features pose difficulties to the flexural rift shoulder mountain model as its support (see Paxman, this volume for discussion of uplift mechanisms).

Using surface wave tomography, Heeszel et al., (2016) found a slow uppermost mantle beneath the Southern TAMS region. They hypothesize that the slow anomaly is either due to the reheating from the WARS activity related to the Terror rift to the north, or evidence of a Cenozoic lithospheric delamination or destruction event. Shen et al., 2018a further improved the images by combining data from Heeszel et al., (2016) together with short period surface wave velocity maps from ambient noise and receiver functions. The updated images show a low velocity zone beneath the southern TAMS in the uppermost mantle (Fig. 8) on top of a dipping high velocity zone (Fig. 9). They suggest that the deeper high velocity zone represents a foundering lithosphere and the LVZ

represents an upwelling asthenosphere, and the system is best interpreted by a lithosphere removal model (Shen et al., 2018a). Beneath the Thiel Mountains and Whitmore Mountains, the same study also identified additional low seismic anomaly in the uppermost mantle, indicative of a thermal origin of these elevated areas in WA.

Although Shen et al., (2018a) showed that the lithosphere has been removed in the Southern TAMS region and provided an estimate of the contribution to uplift from the mantle thermal effect due to the lithosphere removal, it is also clear that the TAMS is complicated and significant alongstrike variation exists. Proposed uplift mechanisms for the TAMS include flexural uplift (ten Brink et al., 1997; Yamasaki, 2008; Wannamaker et al., 2017), thermal mantle support (Lawrence et al., 2006c; Brenn et al., 2017), and crustal thickness and density variations (Bialas et al., 2007; Huerta, 2007). As an example of along-strike variation, a recent magnetotelluric (MT) study by Wannamaker et al. (2017) shows that in the Central TAM, cratonic lithosphere extends nearly up to the TAMS rangefront. Cantilevered flexural uplift appears to be the preferred uplift mechanism and the thermal contribution from the mantle seems smaller in this region. These differences between the Southern and Central TAMS are consistent with the range morphology, in which the Southern TAMS form a large plateau area whereas the Central TAMS form a much narrower mountain range. Indeed, such structural and morphological variability is evident along the full length of the TAMS (Shen et al., 2018; Lloyd et al., 2020).

West Antarctica

The upper mantle structure of West Antarctica is broadly similar to other regions worldwide that have experienced Mesozoic and Cenozoic tectonic activity, such as Western North America. This structure includes shallow Moho depth (Fig. 5), thin lithosphere, and slow upper mantle shear wave velocities in many places (Fig. 6). These characteristics are consistent with the geological history of West Antarctica, which includes rifting in the Weddell Sea Embayment (Jordan et al., 2017) as well as the rotation and translation of the Ellsworth-Whitmore Mountain block during the Jurassic (Grunow et al., 1987), and Cretaceous extension between the West Antarctic crustal block and Zealandia (e.g., Siddoway, 2008; Wobbe et al., 2012). The latter events culminated in the regional cessation of subduction along the margin of Marie Byrd Land. However, subduction continued from Thurston Island to the Antarctic Peninsula, where it gradually ceased from south to north during the Cenozoic (Eagles et al., 2004). The extended continental crust of the WARS underwent further episodes of focused extension during the Cenozoic (Granot et al., 2013; Davey et al., 2016).

The eastern Ross Embayment, central West Antarctica, and the Weddell Sea show modest upper mantle velocity anomalies, with velocities about 1-2% slower than the global average reference velocity (Fig. 4, 6, 11). Mantle seismic velocities increase eastward across the Ross Embayment, consistent with the increase in lithospheric age from the late Cenozoic rifting in the western Ross Embayment (Fielding et al., 2008) to early Cenozoic and Cretaceous lithosphere in the east (Wilson and Luyendyk, 2009). Although aerogeophysical evidence suggests that the boundary between crust of East and West Antarctic affinities occurs in the middle of the Ross Embayment (Tinto et al, 2019), from a seismic structure and tectonics standpoint the boundary occurs along the TAMS. Detailed surface wave results show that the structure of the WARS consists of higher velocity lithospheric mantle extending to depths of about 70-80 km, with lower velocities beneath (Heeszel et al., 2016; O'Donnell et al, 2017; Shen et al., 2018), consistent with cooling since the major extensional episodes

during the Mesozoic and early Cenozoic (Siddoway, 2008; Granot et al., 2013). Some smaller regions show lower velocities, possibly delineating the locus of limited late Cenozoic extension (Lloyd et al., 2015). The Weddell Sea and areas beneath the Ronne Ice Shelf show upper mantle velocities intermediate between the fast EA Lithosphere and the lower velocities in other regions of WA (Fig. 6, 11). This is consistent with age of the lithosphere in this region, dating to the Mesozoic opening of Gondwana (Jordan et al., 2013; 2017).

Shear wave splitting measurements indicate large shear wave splitting times (> 1 s.) in the southern WARS (Fig. 2). The splitting measurements show very consistent fast directions approximately perpendicular to the strike of the nearby Whitmore Mountains and other topographic features, and parallel to likely extension directions for the WARS opening. This strong upper mantle azimuthal anisotropy is interpreted as resulting from lattice preferred orientation induced by asthenospheric mantle strain associated with Cenozoic extension of the WARS (Accardo et al., 2014).

Marie Byrd Land (MBL), an elevated volcanic dome with 18 major subaerial shield and stratovolcanoes (LaMasurier and Rex, 1989), is underlain by low mantle velocities (Fig. 6, 10). Late Quaternary alkaline volcanism at Mt. Berlin and Mt. Takahae (Wilch et al., 1999), and an inferred subglacial magmatic system near Mt. Waesche (Lough et al., 2014) demonstrate current volcanic activity. The crustal thickness of about 30-33 km (Fig 5) is somewhat greater than the surrounding regions (around 25-28 km), but this is not sufficient to explain the elevated topography, suggesting that the elevation is partially supported by a low density thermal anomaly in the uppermost mantle (Chaput et al., 2014; Shen et al., 2018). Several previous studies have proposed a mantle plume origin for the MBL dome, based on the elevated topography and volcano chemistry and petrology (Hole and LaMasurier, 1994; LaMasurier and Landis, 1996; Behrendt, 1999; Panter et al., 2000). Subaerial volcanic peaks are located along linear arrays, in many cases with age progressions, but directions of propagation are not consistent between difference lines, suggesting that the linear trends may be controlled by pre-existing fractures (LaMasurier and Rex, 1989; Paulson and Wilson, 2010) rather than relative motion between the Antarctic plate and the mantle plume. Alternatively, Finn et al., [2005] propose that much of the volcanism of WA results from the volatile-enhanced melting of metasomatized lithosphere formed during Mesozoic subduction along this margin.

Both body (Hansen et al., 2014; Lloyd et al., 2015) and surface wave (Heeszel et al, 2016; Shen et al., 2018) tomography studies show low velocities in the upper mantle beneath the MBL dome. The surface wave results show the existence of a higher velocity mantle lithosphere to depths of 60-80 km, underlain by lower seismic velocities. Methods with good sensitivity to mid-mantle depths generally show low velocity anomalies beneath the MBL dome in the transition zone and upper part of the lower mantle. Fig. 10 compares the results from P-wave tomography (Hansen et al., 2014) and adjoint tomography (Lloyd et al, 2020), with both results showing low velocities in the mid-mantle beneath the MBL dome. The P-wave tomography has almost no resolution of the coastal and oceanic regions due to lack of seismic stations resulting in poor ray-path coverage, but the adjoint tomography which has good resolution shows that the low upper mantle velocities extend past the MBL coastline to a low velocity anomaly at depths of 150-350 km beneath the Amundsen Sea.

The tomography results are consistent with a thermal plume extending at least from the midmantle to the surface beneath MBL. The velocity anomalies are most easily interpreted in terms of

warmer mantle temperatures, as the effects of water on seismic velocities are uncertain and recent laboratory results suggest that water has an insignificant effect on upper mantle seismic velocities (Cline et al., 2018). The magnitude of the shear velocity anomaly is consistent with a 150°C upper mantle thermal anomaly, which can explain the excess topography (Lloyd et al., 2015). The continuity of the slow velocity anomalies from depths of 80 to 800 km is highly suggestive of a mantle plume originating from the mid mantle or deeper, consistent with geochemical evidence (e.g., Panter et al., 2000; Handler et al, this volume). However, the connection between the MBL anomaly and the offshore anomaly, as well as the diverse geographic trends of the volcanic lines, suggests the possibility of a more complicated geodynamical situation than indicated by the classical simple vertical plume model. Simulations of mantle plumes in global mantle flow models suggest that plumes originating at the edge of the Pacific Large Low Shear Velocity Province (LLSVP) at the core-mantle boundary beneath the South Pacific would be tilted southward by the mantle wind, possibly explaining the MBL and offshore seismic anomalies (Bredow and Steinberger, this volume).

Slow upper mantle velocity anomalies extend from the MBL coast through the Amundsen Sea Embayment, and northward along the Antarctic Peninsula (Fig. 11). Along the MBL and Amundsen Sea coastlines, slow velocities extend from the bottom of the thin lithosphere (70 km) to at about 200 km depth, beneath late Pleistocene to recent volcanoes such as Mt Siple in MBL (Wilch et al., 1999) and Mt Hudson (Corr and Vaughn, 2008) near the Amundsen Sea Embayment. The anomalies deepen to 150 to 300 km depth offshore beneath 90 Ma oceanic lithosphere formed during the separation of Zealandia from Antarctica (Eagles et al., 2004), where an extensive shallow bathymetric anomaly is found (Wobbe et al., 2014). The seismic and bathymetric anomalies may result from warm upper mantle near the region where spreading originated between Zealandia and Antarctica, in which the initiation of spreading has been attributed to a mantle plume (Weaver et al., 1994). The presence of low viscosity hydrous mantle material resulting from the long-lived Mesozoic subduction zone that preceded the rifting along the northern Antarctic margin may also play a role (Finn et al., 2005; Sutherland et al., 2010).

Slow seismic anomalies beneath the Antarctic Peninsula are limited to depths shallower than 200 km, and are underlain by fast velocities to the north, in contrast to MBL and the Amundsen Sea regions (Fig 11). This region was the site of subduction of the Phoenix plate beneath Antarctica during the Mesozoic, with subduction ending from South to North during the Cenozoic as the Phoenix-Antarctic spreading center was subducted (Eagles et al., 2004). The fast velocities found in the transition zone beneath the northern peninsula may represent the remnants of the subducted Phoenix slab. As the subducting ridge traversed northward along the peninsula, it formed a slab window in its wake. Slab windows are generally accompanied by erosion of the overriding plate lithosphere and its replacement with hot upwelling asthenosphere (Groome and Thorkelson, 2009). We interpret the slow seismic velocities extending along the entire length of the western margin of the peninsula as due to the effects of the slab window, consistent with the location and limited depth extent of the anomalies.

The slow mantle velocities beneath MBL, the Amundsen Sea Embayment, and the Antarctic Peninsula imply warm upper mantle temperatures, with important implications for ice sheet models and projections of the future of the Antarctic ice sheet. Heat flow estimates, based on the seismic structure, show relatively high geothermal heat flux in these regions (Shen et al., 2020), influencing

water production and drag at the base of the ice sheet (Pollard et al., 2005; Pattyn, 2010). Warm mantle temperatures also imply low mantle viscosity, which predicts short glacial isostatic adjustment timescales that may have important influences on the evolution of the Antarctic ice sheet (Gomez et al, 2015; Whitehouse et al. 2019). The relationship between Antarctic seismic structure, mantle viscosity, and glacial isostatic adjustment is discussed further in Ivins et al (this volume).

Conclusions and Prospects for Future Work

The deployment of numerous seismic stations and the development of new seismic analysis tools over the last two decades has led to great improvements in our knowledge of the upper mantle structure beneath Antarctica. Analysis of empirical Green's Functions from ambient noise correlation allows much better resolution of surface wave dispersion curves at short periods. Bayesian Monte Carlo inversion methods can be used to determine the structure that best fits constraints from multiple types of seismic data, and also provide uncertainty estimates. Adjoint inversion methods, combined with numerical calculations of full waveform synthetic seismograms in 3-D structures, allows the determination of higher resolution structure models of the entire Antarctic continent and surrounding regions throughout the upper mantle and transition zone.

Seismic structure models calculated with these methods now have sufficient resolution to provide important insights into the geological history of the continent. EA shows thick continental mantle lithosphere similar to other Archean and Early Proterozoic terranes on other continents. The fast shear velocities of the lithosphere down to greater than 200 km depth are interpreted as resulting from cold mantle temperatures, and to a lesser extent from chemical depletion, based on studies from other cratonic regions. The deepest and largest lithospheric velocity anomalies occur along a band extending almost entirely across Antarctica 500-1000 inboard from the TAM, probably representing a "Mawson Continent" that formed the core of ancient cratonic lithosphere around which other terranes accreted. Some other regions of EA, notably the Dronning Maud Land highlands and the Lambert Graben region, show much thinner lithosphere, indicating thermal modification of the lithosphere during the Phanerozoic.

The TAMS Front represents a major boundary in the mantle between thick cratonic lithosphere in EA and much thinner lithosphere in WA. In the Ross Embayment region, it is flanked by the late-Cenozoic rifts, which are underlain by an extensive low velocity upper mantle anomaly extending from the mid-ocean ridges north of Antarctica to the southern TAM. This velocity anomaly results from warm mantle along the trace of the rift, which persists even though extension has now apparently ceased. The TAMS show major structural variations along-strike, with the broad Southern TAMS underlain at shallow mantle depths by low seismic velocities indicating an absence of lithospheric mantle, consistent with uplift as a result of lithospheric removal. In contrast, the much narrower Central TAMS is underlain by a sharp boundary between slow WA and fast EA mantle, consistent with classical rift shoulder or flexural uplift models.

The upper mantle seismic structure of WA is dominated by large slow velocity anomalies beneath central MBL, and along the Pacific coastline from MBL through the Antarctic Peninsula. The central MBL anomaly extends through the transition zone, and may represent the thermal anomaly resulting from a mantle plume. Slow velocities beneath the Amundsen Sea Coast link to deeper anomalies offshore, suggesting a connection with deeper mantle processes to the north. Slow anomalies beneath the Antarctic Peninsula are limited to depths shallower than 200 km, and likely

represent thermal anomalies resulting from the erosion of continental lithosphere and replacement by warm mantle during subduction of the Antarctic-Phoenix spreading center.

Continuing work over the next decade should result in higher resolution seismic images of mantle structure, due to improvements in both data collection and seismic analysis. Technological improvements should permit the deployment of denser arrays of seismic stations, as well as deployment of stations in regions without previous instrumentation. The development of much smaller and lighter autonomous seismic stations with more reliable power supplies should facilitate deployment in remote parts of the continent. Better and lower-cost satellite communications should allow real-time transmission of seismic data from remote sites, and also reduce the cost of operation by reducing the need for maintenance visits. An international effort is needed to instrument the vast regions of EA that are so far without any seismograph deployments.

Improvements in data analysis will also allow advances to take place using existing data. Surface wave data can be analyzed to yield better constraints on anisotropy. Combined analysis of Love and Rayleigh waves will yield estimates on the variations of radial seismic anisotropy, the difference between vertically and horizontally polarized shear waves (O'Donnell et al., 2019; Zhou et al, 2019). Analysis of Rayleigh wave phase velocities for azimuthal anisotropy will allow resolution of the depth distribution of azimuthal anisotropy, which is poorly constrained by SKS analysis. The resulting maps of the lateral and depth distribution of azimuthal anisotropy will provide important constraints on the distribution and orientation of mantle fabric, due to either past tectonic processes or current mantle deformation and flow. Improved techniques will also increase the resolution of isotropic structural variations. Double difference tomography, which uses the differences in waveforms from the same earthquake recorded at different seismic stations, will improve resolution on the Antarctic continent by localizing the structure kernels in the vicinity of the stations (Yuan et al., 2016). The incorporation of Green's Functions from ambient noise cross correlation into adjoint tomography will also increase resolution (Chen et al., 2013; Liu et al., 2017). With the continued improvement of datasets and analysis methods, future seismic studies of the Antarctic mantle will provide important new insights into the geological history and current geodynamic processes of Antarctica.

References

Accardo, N. J., D. A. Wiens, S. Hernandez, R. C. Aster, A. Nyblade, A. Huerta, S. Anandakrishnan, T. Wilson, D. S. Heeszel and I. W. D. Dalziel, Upper mantle seismic anisotropy beneath the West Antarctic Rift System and surrounding region from shear wave splitting analysis, *Geophys. J. Int.*, **198**, 414–429, doi: 10.1093/gji/ggu117, 2014

Ammon, C., (1991). The isolation of receiver effects from teleseismic P waveforms, Bull. Seis. Soc. Am., 81, 2504-2510.

An, M., D. A. Wiens, Y. Zhao, M. Feng, A. A. Nyblade, M. Kanao, Y. Li, A. Maggi, and J.-J. Lévêque (2015), S-velocity model and inferred Moho topography beneath the Antarctic Plate from Rayleigh waves, J. Geophys. Res. Solid Earth, 120, 359–383, doi:10.1002/2014JB011332.

Anandakrishnan, A., D. E. Voigt, P. G. Burkett, and R. Henry, Deployment of a broadband seismic network in west Antarctica, Geophys. Res. Lett., 27, 2053–2056, 2000.

Baker MG, Aster RC, Anthony RE, Chaput J, Wiens DA, Nyblade A, Bromirski PD, Gerstoft P, Stephen RA (2019). Seasonal and spatial variations in the ocean-coupled ambient wavefield of the Ross Ice Shelf. Journal of Glaciology 1–14. https://doi.org/10.1017/jog.2019.64

Bannister, S., J. Yu, B. Leitner, and B. L. N. Kennett, Variations in crustal structure across the transition from West to East Antarctica, Southern Victoria Land, *Geophys. J. Int.* (2003) 155, 870–884, 2003

Barklage, M., Wiens, D.A., Nyblade, A. & Anandakrishnan, S., 2009. Upper mantle seismic anisotropy of South Victoria Land and the Ross Sea coast, Antarctica from SKS and SKKS splitting analysis, *Geophys. J. Int.*, **178**, 729–741.

Bayer, B., Muller, C., Eaton, D.W. & Jokat, W., 2007. Seismic anisotropy beneath Dronning Maud Land, Antarctica, revealed by shear wave splitting, *Geophys. J. Int.*, **171**, 339–351.

Behrendt, J. C. (1999), Crustal and lithospheric structure of the West Antarctic Rift System from geophysical investigations—A review, Global Planet. Change, 23(1), 25–44.

Bentley, C., 1973. Crustal structure of Antarctica. Tectonophysics 20, 229–240.

Bernacchi, L.C. & Milne, J., 1908. Earthquakes and other earth movements recorded in the Antarctic regions, 1902-1903, in National Antarctic Expedition 1901-1904. Physical Observations. London, Royal Society, 1908, pp 37-96.

Bialas, R.W., Buck, W.R., Studinger, M., and Fitzgerald, P.G., 2007, Plateau collapse model for the Transantarctic Mountains—West Antarctic Rift System: Insights from numerical experiments: Geology, v. 35, p. 687–690 https://doi.org/10.1130/G23825A.1.

Bina, C. R., and G. Helffrich, 1994, Phase transition Clapeyron slopes and transition zone seismic discontinuity topography, *J. Geophys. Res.*, *99*, 15853-15860.

Brenn, G. R., S. E. Hansen, and Y. Park, Variable thermal loading and flexural uplift along the Transantarctic Mountains, Antarctica, Geology, 45, 463-466, 2017.

Boger, S. D. (2011), Antarctica—Before and after Gondwana, Precambrian Res., 19, 335–371, doi:10.1016/j.gr.2010.09.003.

Bozdağ, E., Peter, D., Lefebvre, M., Komatitsch, D., Tromp, J., Hill, J., et al. (2016). Global adjoint tomography: First-generation model. Geophysical Journal International, 207(3), 1739–1766. https://doi.org/10.1093/gji/ggw356

Brommer, A., Millar, I.L., Zeh, A., 1999. Geochronology, structural geology and petrography of the northwestern La Grange Nunataks, Shackleton Range, Antarctica. Terra Antarctica 6, 269–278.

Chaput, J., R. Aoster, A. Huerta, X. Sun, A. Lloyd, D. Wiens, A. Nyblade, S. Anandakrishnan, J. Winberry, and T. Wilson The crustal thickness of West Antarctica. Journal of Geophysical Research: Solid Earth, 119(1), pp.378-395 (2014).

- Chang, S.-J., C.-E. Baag, and C. A. Langston (2004), Joint Analysis of Teleseismic Receiver Functions and Surface Wave Dispersion using the Genetic Algorithm, Bull. Seism. Soc. Am., 94, 691–704.
- Cline, C. J., U. H. Faul, E. C. David, A. J. Berry, and I. Jackson, 2018. Redox-influenced seismic properties of upper- mantle olivine, Nature, 555, 355-358.
- Corr, H. F., & Vaughan, D. G. (2008). A recent volcanic eruption beneath the West Antarctic ice sheet. Nature Geoscience, 1(2), 122–125. https://doi.org/10.1038/ngeo106
- Danesi, S., and A. Morelli (2001), Structure of the upper mantle under the Antarctic Plate from surface wave tomography, Geophys. Res. Lett., 28, 4395 4398.
- Davey, F. J., R. Granot, S. C. Cande, J. M. Stock, M. Selvans, and F. Ferraccioli (2016), Synchronous oceanic spreading and continental rifting in West Antarctica, Geophys. Res. Lett., 43, 6162–6169, doi:10.1002/2016GL069087.
- Day, J. M. D., R. P. Harvey, and D. R. Hilton (2019). Melt-modified lithosphere beneath Ross Island and its role in the tectono-magmatic evolution of the West Antarctic Rift System, Chemical Geology, 518, 45-54.
- Eagles, G., Gohl, K., & Larter, R. D. (2004). High-resolution animated tectonic reconstruction of the South Pacific and West Antarctic margin. Geochemistry, Geophysics, Geosystems, 5, Q07004. https://doi.org/10.1029/2003GC000657
- Emry, E.L., Nyblade, A.A., Julià, J., Anandakrishnan, S., Aster, R.C., Wiens, D.A., Huerta, A.D., and Wilson, T.J., 2015, The mantle transition zone beneath West Antarctica: Seismic evidence for hydration and thermal upwellings: Geochemistry, Geophysics, Geosystems, v. 15, doi: 10.1002/2014GC005588
- Emry, E. L., A. A. Nyblade, A. Horton, S. E. Hansen, J. Julià, R. C. Aster, A. D. Huerta, J. P. Winberry, D. A. Wiens, S. Anandakrishnan, and T. J. Wilson, Prominent thermal anomalies in the mantle transition zone beneath the Transantarctic Mountains, Geology, in press, 2020.
- Ferraccioli, F., C. A. Finn, T. A. Jordan, R. E. Bell, L. M. Anderson, and D. Damaske (2011), East Antarctic rifting triggers uplift of the Gamburtsev Mountains, Nature, 479, 388–392, doi:10.1038/nature10566.
- Fielding, C. R., J. Whittaker, S. A. Henrys, T. J. Wilson, and T. R. Naish (2008), Seismic facies and stratigraphy of the Cenozoic succession in McMurdo Sound, Antarctica: Implications for tectonic, climatic and glacial history, Palaeogeogr. Palaeoclimatol. Palaeoecol., 260(1), 8–29.
- Finn, C. A., R. D. Müller, and K. S. Panter (2005), A Cenozoic diffuse alkaline magmatic province (DAMP) in the southwest Pacific without rift or plume origin, Geochem. Geophys. Geosyst., 6, Q02005, doi:10.1029/2004GC000723.

- Fichtner, A., Kennett, B. L., Igel, H., & Bunge, H. P. (2009). Full seismic waveform tomography for upper-mantle structure in the Australasian region using adjoint methods. Geophysical Journal International, 179(3), 1703–1725. https://doi.org/10.1111/j.1365-246X.2009.04368.x
- Fitzsimons, I. C. W. (2000). A review of tectonic events in the East Antarctic shield and their implications for Gondwana and earlier supercontinents. Journal of African Earth Sciences, 31(1), 3–23. https://doi.org/10.1016/S0899-5362(00)00069-5
- Foley, S. F., A.V. Andronikov, D.E. Jacob, S. Melzer, (2006). Evidence from Antarctic mantle peridotite xenoliths for changes in mineralogy, geochemistry and geothermal gradients beneath a developing rift, Geochimica et Cosmochimica Acta 70, 3096–3120.
- Forsyth, D.W. and Li, A., (2005). Array analysis of two-dimensional variations in surface wave phase velocity and azimuthal anisotropy in the presence of multipathing interference, in Seismic Earth: Array Analysis of Broadband Seismograms, Geophys. Mono. Series, 157, 81-97.
- French, S.W., Romanowicz, B., 2015. Broad plumes rooted at the base of the Earth's mantle beneath major hotspots. Nature 525, 95–99. https://doi.org/10.1038/ nature14876.
- Gomez, N., D. Pollard, D. Holland, Sea-level feedback lowers projections of future Antarctic ice sheet mass loss. *Nat. Commun.* 6:8798 doi: 10.1038/ncomms9798, 2015.
- Goodge, J.W., Fanning, C.M., 1999. 2.5 b.y. of punctuated Earth history as recorded in a single rock. Geology 27, 1007–1010.
- Goodge, J. W., Fanning, C. M., & Bennett, V. C. (2001). U–Pb evidence of ~1.7 Ga crustal tectonism during the nimrod orogeny in the Transantarctic Mountains, Antarctica: Implications for Proterozoic plate reconstructions. Precambrian Research, 112(3-4), 261–288, https://doi.org/10.1016/S0301-9268(01)00193-0
- Goodge, J. W. and Fanning, C. M.: Mesoarchean and Paleoproterozoic history of the Nimrod Complex, central Transantarctic Mountains, Antarctica: Stratigraphic revisions and relation to the Mawson Continent in East Gondwana, Precambrian Res., 285, 242–271, https://doi.org/10.1016/j.precamres.2016.09.001, 2016.
- Goodge, J. W., Fanning, C. M., Fisher, C. M., and Vervoort, J. D.: Proterozoic crustal evolution of central East Antarctica: Age and isotopic evidence from glacial igneous clasts, and links with Australia and Laurentia, Precambrian Res., 299, 151–176, https://doi.org/10.1016/j.precamres.2017.07.026, 2017.
- Granot, R., Cande, S. C., Stock, J. M., & Damaske, D. (2013). Revised Eocene-Oligocene kinematics for the West Antarctic rift system. Geophysical Research Letters, 40, 279–284. https://doi.org/10.1029/2012GL054181
- Granot, R. and J. Dyment (2018). Late Cenozoic unification of East and West Antarctica, Nature Communications, 9:3189, DOI: 10.1038/s41467-018-05270

- Graw J. H., A. N. Adams, S. E. Hansen, D. A. Wiens, L. Hackworth, Y. Park, Upper mantle shear wave velocity structure beneath northern Victoria Land, Antarctica: Volcanism and uplift in the northern Transantarctic Mountains, *Earth Planet. Sci. Lett.*, 449, 48-60, 2016.
- Groome, W. G., & Thorkelson, D. J. (2009). The three-dimensional thermo-mechanical signature of ridge subduction and slab window migration. Tectonophysics, 464(1-4), 70–83. https://doi.org/10.1016/j.tecto.2008.07.003
- Grunow, AM., D.V. Kent, and I.W.D. Dalziel. 1987. Mesozoic evolution of West Antarctica and the Weddell Sea basin: New paleomagnetic constraints. *Earth and Planetary Science Letters*. 86, 16-26.
- Hansen, S. E., A. A. Nyblade, D. S. Heeszel, D. A. Wiens, P. Shore, M. Kanao, Crustal structure of the Gamburtsev Mountains, East Antarctica, from S-wave receiver functions and Rayleigh wave phase velocities, *Earth Planet. Sci. Lett.*, *300*, 395-401, 2010.
- Hansen, S. E., J. H. Graw, L. M. Kenyon, A. A. Nyblade, D. A. Wiens, R. C. Aster, A. D. Huerta, S. Anandakrishnan, T. Wilson, Imaging the Antarctic mantle using adaptively parameterized P-wave tomography: Evidence for heterogeneous structure beneath West Antarctica, *Earth Planet. Sci. Lett.*, 408, 66–78, 2014.
- Hansen, S.E., A. M. Reusch, T. Parker, D. K. Bloomquist, P. Carpenter, J. H. Graw, and G. R. Brenn, The Transantarctic Mountains Northern Network (TAMNNET): Deployment and Performance of a Seismic Array in Antarctica, Seism. Res. Lett., 86, 1636 1644, 2015.
- Heeszel, D. S., D. A. Wiens, A. A. Nyblade, S. E. Hansen, M. Kanao, M. An, and Y. Zhao, Rayleigh wave constraints on the structure and tectonic history of the Gamburtsev Subglacial Mountains, East Antarctica, *J. Geophys. Res.*, 118, doi:10.1002/jgrb.50171, 2013.
- Heeszel, D. S., D.A.Wiens, S. Anandakrishnan, R. C. Aster, I. W. D. Dalziel, A. D. Huerta, A. A. Nyblade, T. J. Wilson, and J. P. Winberry, Upper mantle structure of central and West Antarctica from array analysis of Rayleigh wave phase velocities, *J. Geophys. Res. Solid Earth*, *121*, doi:10.1002/2015JB012616, 2016.
- Hole, M.J., LeMasurier, W.E., 1994. Tectonic controls on the geochemical composition of Cenozoic mafic alkaline volcanic rocks from West Antarctica. Contributions to Mineralogy and Petrology, 117(2): 187-202.
- Huerta, A.D., 2007, Lithospheric Structure across the Transantarctic Mountains constrained by analysis of gravity and thermal structure: In: Antarctica: A Keystone in a Changing World. Cooper, A., and C. Raymond, eds. U.S.G.S. Open-File Report 2007-1047
- Ivins, E.R., James, T.S., 2005. Antarctic glacial isostatic adjustment: a new assess- ment. Antarct. Sci. 17 (4), 537–549.
- Ivins, E.R., Sammis, C.G., 1995. On lateral viscosity contrast in the mantle and the rheology of low-frequency geodynamics. Geophys. J. Int. 123 (2), 305–322.
- Jordan, T. H., 1981. Continents as a chemical boundary layer, Phil. Trans. R. Soc. Long. A., 301, 359-3783.

Jordan T. A., F. Ferraccioli, N. Ross, H. F.J. Corr, P. T. Leat, R. G. Bingham, D. M. Rippin, A. le Brocq, M. J. Siegert, Inland extent of the Weddell Sea Rift imaged by new aerogeophysical data, Tectonophysics, 585, 137-160, 2013.

Jordan, T. A., F. Ferraccioli, and P. T. Leat (2017), New geophysical compilations link crustal block motion to Jurassic extension and strike-slip faulting in the Weddell Sea Rift System of West Antarctica, Gondwana Res, 42, 29-48.

Karato, S., Jung, H., Katayama, I. & Skemer, P., 2008. Geodynamic significance of seismic anisotropy of the upper mantle: new insights from laboratory studies, *Annu. Rev. Earth planet. Sci.*, **36**, 59–95.

Komatitsch, D., & Tromp, J. (1999). Introduction to the spectral element method for three-dimensional seismic wave propagation. Geophysical Journal International, 139(3), 806–822. https://doi.org/10.1046/j.1365-246x.1999.00967.x

Komatitsch, D., & Tromp, J. (2002a). Spectral-element simulations of global seismic wave propagation—I. Validation. Geophysical Journal International, 149(2), 390–412. https://doi.org/10.1046/j.1365-246X.2002.01653.x

Komatitsch, D., & Tromp, J. (2002b). Spectral-element simulations of global seismic wave propagation—II. Three-dimensional models, oceans, rotation and self-gravitation. Geophysical Journal International, 150(1), 303–318. https://doi.org/10.1046/j.1365-246X.2002.01716.x

Komatitsch, D., & Vilotte, J. P. (1998). The spectral element method: An efficient tool to simulate the seismic response of 2D and 3D geological structures. Bulletin of the Seismological Society of America, 88(2), 368–392.

Kustowski, B., Ekström, G., & Dziewoński, A. M. (2008). Anisotropic shear-wave velocity structure of the Earth's mantle: A global model. Journal of Geophysical Research - Solid Earth, 113. https://doi.org/10.1029/2007JB005169

Kyle, P.R., 1990. McMurdo Volcanic Group — Western Ross Embayment: Introduction. In: LeMasurier, W.E., Thomson, J.W. (Eds.), Volcanoes of the Antarctic Plate and Southern Oceans. Antarctic Research Series, vol. 48. American Geophysical Union, Washington, D.C., pp. 19–25.

Kyle, P.R., Moore, J.A., Thirlwall, M.F., 1992. Petrologic evolution of anorthoclase phonolite lavas at Mount Erebus, Ross Island, Antarctica. J. Petrol. 33, 849–875. https://doi.org/10.1093/petrology/33.4.849.

Leitchenkov, G., Kudryavtzev, G., 1997. Structure and origin of the Earth's Crust in the Weddell Sea Embayment (beneath the Front of the Filchner and Ronne Ice Shelves) from deep seismic sounding data. Polarforschung 67(3):143–154.

Lawrence, J. F., and D. A. Wiens, Combined receiver function and surface wave phase velocity inversion using a niching genetic algorithm: Application to Patagonia, *Bull, Seism. Soc. Am., 94*, 977-987, 2004.

- Lawrence, J. F., Wiens, D. A., Nyblade, A. A., Anandakrishnan, S., Shore, P. J., & Voigt, D. (2006a). Rayleigh wave phase velocity analysis of the Ross Sea, Transantarctic Mountains, and East Antarctica from a temporary seismograph array. Journal of Geophysical Research Solid Earth, 111. https://doi.org/10.1029/2005JB003812
- Lawrence, J. F., Wiens, D. A., Nyblade, A. A., Anandakrishan, S., Shore, P. J., & Voigt, D. (2006b). Upper mantle thermal variations beneath the Transantarctic Mountains inferred from teleseismic S-wave attenuation. Geophysical Research Letters, 33, L03303. https://doi.org/10.1029/2005GL024516
- Lawrence, J. F., D. A. Wiens, A. A. Nyblade, S. Anandakrishnan, P. J. Shore, and D. Voigt (2006c), Crust and upper mantle structure of the Transantarctic Mountains and surrounding regions from receiver functions, surface waves, and gravity: Implications for uplift models, Geochem. Geophys. Geosyst., 7, Q10011, doi:10.1029/2006GC001282.
- Laske, G., Masters, G., Ma, Z., & Pasyanos, M. (2013). Update on CRUST1.0—A 1-degree global model of Earth's crust. Geophys. Res. Abstr, 15, Abstract EGU2013-2658
- Lee, C.-T. A., Compositional variation of density and seismic velocities in natural peridotites at STP conditions: Implications for seismic imaging of compositional heterogeneities in the upper mantle, J. Geophys. Res., 108(B9), 2441, doi:10.1029/2003JB002413, 2003.
- LeMasurier, W.E., Rex, D.C., 1989. Evolution of linear volcanic ranges in Marie Byrd Land, West Antarctica. Journal of Geophysical Research: Solid Earth, 94(B6): 7223-7236.
- LeMasurier, W.E., Landis, C.A., 1996. Mantle-plume activity recorded by low-relief erosion surfaces in West Antarctica and New Zealand. Geological Society of America Bulletin, 108(11): 1450-1466.
- Levander, A., Schmandt, B., Miller, M.S., Liu, K., Karlstrom, K.E., Crow, R.S., Lee, C.-T.A., and Humphreys, E.D., 2011, Continuing Colorado Plateau uplift by delamination-style convective lithospheric downwelling: Nature, v. 472, p. 461–465, https://doi.org/10.1038/nature10001.
- Licht, K. J., Groth, T., Townsend, J. P., Hennessy, A. J., Hemming, S. R., Flood, T. P., & Studinger, M. (2018). Evidence for extending anomalous Miocene volcanism at the edge of the East Antarctic craton. Geophysical Research Letters, 45(7), 3009–3016. https://doi.org/10.1002/2018GL077237
- Liu, Y., Niu, F., Chen, M., & Yang, W. (2017). 3-D crustal and uppermost mantle structure beneath NE China revealed by ambient noise adjoint tomography. *Earth and Planetary Science Letters*, *461*, 20-29.
- Lloyd, A. J. (2018) Seismic Tomography of Antarctica and the Southern Oceans: Regional and
- Continental Models from the Upper Mantle to the Transition Zone, Ph.D. Thesis, Washington University in St Louis, St. Louis, MO, 175 pp.
- Lloyd, A. J., A. A. Nyblade, D. A. Wiens, S. E. Hansen, M. Kanao, P. J. Shore, and D. Zhao, Upper mantle seismic structure beneath central East Antarctica from body wave tomography: Implications for the origin of the Gamburtsev Subglacial Mountains, *Geochem. Geophys. Geosyst.*, *14*, 10.1002/ggge.20098, 2013.
- Lloyd, A. J., D. A. Wiens, A. A. Nyblade, S. Anandakrishnan, R. C. Aster, A. D. Huerta, T. J. Wilson, I. W. D. Dalziel, P. J. Shore, and D. Zhao, A seismic transect across West Antarctica: Evidence for

- mantle thermal anomalies beneath the Bentley Subglacial Trench and the Marie Byrd Land Dome, *J. Geophys. Res. Solid Earth, 120,* 8439–8460, doi:10.1002/2015JB012455, 2015.
- Lloyd, A. J., Wiens, D. A., Zhu, H., Tromp, J., Nyblade, A. A., Aster, R. C., et al (2020). Seismic structure of the Antarctic upper mantle imaged with adjoint tomography. Journal of Geophysical Research: Solid Earth, 124. https://doi.org/10.1029/2019JB017823
- Lough, A. C., D. A. Wiens, C. G. Barcheck, S. Anandakrishnan, R. C. Aster, D. D. Blankenship, A. D. Huerta, A. Nyblade, D. A. Young, and T. J. Wilson, Seismic detection of an active subglacial magmatic complex in Marie Byrd Land, Antarctica, *Nature Geoscience*, *6*, 1031-1035, 2013.
- Lucas, E. M. Lucas, D. Soto, A. A. Nyblade, A. J. Lloyd, R. C. Aster, D. A. Wiens, J. P. O'Donnell, G. W. Stuart, T. J. Wilson, I. W. Dalziel, J. P. Winberry, A. D. Huerta, P- and S-wave velocity structure of central West Antarctica: Implications for the tectonic evolution of the West Antarctic Rift System, Earth Planet. Sci. Lett., in press, 2020.
- Mainprice, D. & Silver, P.G., 1993. Interpretation of SKS-waves using samples from the subcontinental lithosphere, *Phys. Earth planet. Inter.*, **78**, 257–280.
- Maritati, A., Danišík, M., Halpin, J. A., Whittaker, J. M., & Aitken, A. R. A. (2020). Pangea rifting shaped the East Antarctic landscape. *Tectonics*, 39, e2020TC006180. https://doi.org/10.1029/2020TC006180
- Martin, A. P., and A. F. Cooper. "Post 3.9 Ma fault activity within the West Antarctic rift system: onshore evidence from Gandalf Ridge, Mount Morning eruptive centre, southern Victoria Land, Antarctica." Antarctic Science 22.5 (2010): 513-521.
- Martin, A. P., and J. L. Smellie, 2020. Erebus Volcanic Province: petrology. In Smellie, J. L., Panter, K. S. and Geyer, A. (eds) 2020. Volcanism in Antarctica: 200 Million Years of Subduction, Rifting and Continental Break-up. Geological Society, London, Memoirs, 55, 1–40,
- Muller, C., 2001. Upper mantle seismic anisotropy beneath Antarctica and the Scotia Sea region, *Geophys. J. Int.*, **147**, 105–122.
- O'Donnell, J. P., Selway, K., Nyblade, A. A., Brazier, R. A., Wiens, D. A., Anandakrishnan, S., et al. (2017). The uppermost mantle seismic velocity and viscosity structure of central West Antarctica. Earth and Planetary Science Letters, 472, 38–49. https://doi.org/10.1016/j.epsl.2017.05.016
- O'Donnell, J. P., G.W. Stuart, A.M. Brisbourne, K. Selway, Y. Yang, G.A. Nield, P.L. Whitehouse, A.A. Nyblade, D.A. Wiens, R.C. Aster, S. Anandakrishnan, A.D. Huerta, T. Wilson, J.P. Winberry, The uppermost mantle seismic velocity structure of West Antarctica from Rayleigh wave tomography: Insights into tectonic structure and geothermal heat flow, Earth Planet Sci Lett, 522, 219–233, 2019a.
- O'Donnell, J. P., Brisbourne, A. M., Stuart, G. W., Dunham, C. K., Yang, Y., Nield, G. A. et al. (2019b). Mapping crustal shear wave velocity structure and radial anisotropy beneath West Antarctica using seismic ambient noise. *Geochemistry, Geophysics, Geosystems*, 20, 5014–5037. https://doi.org/10.1029/2019GC008459

- Oliver, R.L., Fanning, C.M., 2002. Proterozoic geology east and southeast of Common-wealth Bay, George V Land, Antarctica, and its relationship to that of adjacent Gondwana terranes. In: Gamble, J.A., Skinner, D.N.B., Henrys, S. (Eds.), Antarctica at the Close of the Millennium: Royal Society of New Zealand, Bulletin, 35, pp. 51–58. Wellington.
- Panter, K. S., S. R. Hart, P. Kyle, J. Blusztanjn, T. Wilch, 2000. Geochemistry of Late Cenozoic basalts from the Crary Mountains: characterization of mantle sources in Marie Byrd Land, Antarctica, Chem Geology, 165, 215-241.
- Panter, K.S., Castillo, P., Krans, S., Deering, C., McIntosh, W., Valley, J.W., Kitajima, K., Kyle, P., Hart, S., Blusztajn, J., 2018. Melt origin across a rifted continental margin: a case for subduction-related metasomatic agents in the lithospheric source of alkaline basalt, northwest Ross Sea, Antarctica. Journal of Petrology: doi: 10.1093/petrology/egy036.
- Pappa, F., Ebbing, J., & Ferraccioli, F. (2019a). Moho depths of Antarctica: Comparison of seismic, gravity, and isostatic results. *Geochemistry, Geophysics, Geosystems*, 20, 1629–1645. https://doi.org/10.1029/2018GC008111
- Pappa, F., Ebbing, J., Ferraccioli, F., & van der Wal, W. (2019b). Modeling satellite gravity gradient data to derive density, temperature, and viscosity structure of the antarctic lithosphere. Journal of Geophysical Research: Solid Earth, 124, 12,053–12,076. https://doi.org/10.1029/2019JB017997
- Pattyn, F. Antarctic subglacial conditions inferred from a hybrid ice sheet/ice stream model. *Earth and Planetary Science Letters*, **295**, 451–461 (2010).
- Paulsen, T. S., and T. J. Wilson (2010), Evolution of Neogene volcanism and stress patterns in the glaciated West Antarctic Rift, Marie Byrd Land, Antarctica, J. Geol. Soc., 167(2), 401–416.
- Phillips, G. & Laufer, A. L. Brittle deformation relating to the Carboniferous–Cretaceous evolution of the Lambert Graben, East Antarctica: A precursor for Cenozoic relief development in an intraplate and glaciated region. Tectonophysics 471, 216–224 (2009).
- Phillips, E. H., Sims, K. W., Blichert-Toft, J., Aster, R. C., Gaetani, G. A., Kyle, P. R., et al. (2018). The nature and evolution of mantle upwelling at Ross Island, Antarctica, with implications for the source of HIMU lavas. Earth and Planetary Science Letters, 498, 38–53. https://doi.org/10.1016/j.epsl.2018.05.049
- Priestley, K., McKenzie, D., 2006. The thermal structure of the lithosphere from shear wave velocities. Earth Planet. Sci. Lett. 244, 285–301.
- Pyle, M. L., D. A. Wiens, A. A. Nyblade, and S. Anandakrishnan, Crustal structure of the Transantarctic Mountains near the Ross Sea from ambient seismic noise tomography, J. Geophys. Res., 115, B11310, doi:10.1029/2009JB007081, 2010.
- Ramirez, C, A. Nyblade, S.E. Hansen, D.A. Wiens, S. Anandakrishnan, R.C. Aster, A.D. Huerta, P. Shore and T. Wilson, Crustal and upper-mantle structure beneath ice-covered regions in Antarctica from *S*-wave receiver functions and implications for heat flow, *Geophys. J. Int.*, *204*, 1636–1648, 2016.

Ramirez, C., A. Nyblade, E.L. Emry, J. Julià, X. Sun, S. Anandakrishnan, D.A. Wiens, R.C. Aster, A.D. Huerta, P. Winberry, T. Wilson; Crustal structure of the Transantarctic Mountains, Ellsworth Mountains and Marie Byrd Land, Antarctica: constraints on shear wave velocities, Poisson's ratios and Moho depths, *Geophys. J. Int.*, *211*, 1328–1340, https://doi.org/10.1093/gji/ggx333, 2017.

Reading, A. M., The seismic structure of Precambrian and early Palaeozoic terranes in the Lambert Glacier region, East Antarctica, Earth Planet Sci Lett, 244, 44–57, 2006

Reading, A.M. & Heintz, M., 2008. Seismic anisotropy of East Antarctica from shear-wave splitting: spatially varying contributions from lithospheric structural fabric and mantle flow? *Earth planet. Sci. Lett.*, **268**, 433–443.

Reusch, A. M., Nyblade, A. A., Benoit, M. H., Wiens, D. A., Anandakrishnan, S., Voigt, D., & Shore, P. J. (2008). Mantle transition zone thickness beneath Ross Island, the Transantarctic Mountains, and East Antarctica. *Geophysical research letters*, 35(12)

Ritzwoller, M. H., N. M. Shapiro, A. L. Levshin, and G. M. Leahy (2001), Crustal and upper mantle structure beneath Antarctica and surrounding oceans, J. Geophys. Res., 106, 30,645–30,670.

Robertson Maurice, S. D., D. A. Wiens, P. J. Shore, E. Vera, and L. M. Dorman, Seismicity and tectonics of the South Shetland Islands and Bransfield Strait from a regional broadband seismograph deployment, J. Geophys. Res., 108(B10), 2461, doi:10.1029/2003JB002416, 2003.

Roult, G., D. Rouland, and J. P. Montagner, Antarctica II: Upper mantle structure from velocities and anisotropy, Phys. Earth Planet. Inter., 84, 33 - 57, 1994.

Savage, M.K., 1999. Seismic anisotropy and mantle deformation: what have we learned from shear wave splitting?, *Rev. Geophys.*, **37**, 65–106.

Schutt, D.L., Lesher, C.E., 2006. Effects of melt depletion on the density and seismic velocity of garnet and spinel lherzolite. J. Geophys. Res. 111, B05401, http://dx.doi.org/10.1029/2003JB002950.

Shapiro, N. M., M. Campillo, L. Stehly, and M. H. Ritzwoller (2005), High-resolution surface wave tomography from ambient seismic noise, Science, 307, 1615–1618.

Shen, W., Wiens, D. A., Stern, T., Anandakrishnan, S., Aster, R. C., Dalziel, I., et al. (2018a). Seismic evidence for lithospheric foundering beneath the southern Transantarctic Mountains, Antarctica. Geology, 46(1), 71–74. https://doi.org/10.1130/G39555.1

Shen, W., D. A. Wiens, S. Anandakrishnan, R. C. Aster, P. Gerstoft, P. D. Bromirski, et al. The crust and upper mantle structure of central and West Antarctica from Bayesian inversion of Rayleigh wave and receiver functions. *J. Geophys. Res: Solid Earth, 123,* 7824–7849. https://doi.org/10.1029/2017JB015346, 2018b.

Shen, W., Wiens, D. A., Lloyd, A. and Nyblade, A. A., (2020). A Geothermal heat flux map of Antarctica empirically constrained by seismic structure. *Geophysical Research Letters*, p.e2020GL086955.

Siddoway, C. S. (2008). Tectonics of the West Antarctic rift system: New light on the history and dynamics of distributed intracontinental extension, in Cooper, A. et al., Antarctica: A Keystone in a Changing World, National Academy of Sciences, Washington, D.C., pp. 91-114.

Sieminski, A., Debayle, E., Lévêque, J.J., 2003. Seismic evidence for deep low-velocity anomalies in the transition zone beneath West Antarctica. Earth Planet. Sci. Lett. 216 (4), 645–661. https://doi.org/10.1016/s0012-821x(03)00518-1.

Silver, P.G., 1996. Seismic anisotropy beneath the continents: probing the depths of geology, *Ann. Rev. Earth planet. Sci.*, **24**, 385–432.

Sleep, N. H., (2005) Evolution of Continental Lithosphere, Annu. Rev. Earth Planet. Sci, 33, 369-393.

Stump, E., Sheridan, M. F., Borg, S. G., & Sutter, J. F. (1980). Early Miocene subglacial basalts, the East Antarctic ice sheet, and uplift of the Transantarctic Mountains. Science, 207(4432), 757–759. https://doi.org/10.1126/science.207.4432.757

Sutherland, R., Spasojevic, S., Gurnis, M., 2010. Mantle upwelling after Gondwana subduction death explains anomalous topography and subsidence histories of eastern New Zealand and West Antarctica. Geology 38 (2), 155–158. http://dx.doi.org/10.1130/ G30613.1.

Swain, G., Woodhouse, A., Hand, M., Barovich, K., Schwarz, M., Fanning, C.M., 2005. Provenance and tectonic development of the late Archaean Gawler Craton, Australia; U–Pb zircon, geochemical and Sm–Nd isotopic implications. Precambrian Research 141, 106–136.

Szwillus, W., Afonso, J. C. C., Ebbing, J., & Mooney, W. D.(2019). Global crustal thickness and velocity structure from geostatistical analysis of seismic data. Journal of Geophysical Research: Solid Earth, 124, 1626–1652. https://doi-org.libproxy.wustl.edu/10.1029/2018JB016593

Tarantola, A. (1984). Inversion of seismic reflection data in the acoustic approximation. Geophysics, 49(8), 1259–1266. https://doi.org/10.1190/1.1441754

Tape, C., Liu, Q., Maggi, A., & Tromp, J. (2010). Seismic tomography of the southern California crust based on spectral-element and adjoint methods. Geophysical Journal International, 180(1), 433–462. https://doi.org/10.1111/j.1365-246X.2009.04429.x

Ten Brink, U.S., S. Bannister, B.C. Beaudoin, and T. A. Stern, Geophysical investigations of the tectonic boundary between East and West Antarctica, Science, 261, 45-50, 1993.

Tingey, R. J. (1991). The regional geology of Archean and Proterozoic rocks in Antarctica. In The geology of Antarctica, (pp. 1–73).

Tinto, K. J., et al., (2019) Ross Ice Shelf response to climate driven by the tectonic imprint on seafloor bathymetry, Nature Geoscience, 12, 441-449, https://doi.org/10.1038/s41561-019-0370-2

Trey, H., Cooper, A., Pellis, G., della Vedova, B., Cochrane, G., Brancolini, G., Makris, J., 1999. Transect across the West Antarctic rift system in the Ross Sea, Antarctica, Tectonophysics 301:61–74.

Tromp, J., Tape, C., & Liu, Q. (2005). Seismic tomography, adjoint methods, time reversal and banana-doughnut kernels. Geophysical Journal International, 160(1), 195–216. https://doi.org/10.1111/j.1365-246X.2004.02453.x

van de Flierdt, T., S. R. Hemming, S. L. Goldstein, G. E. Gehrels, and S. E. Cox (2008), Evidence against a young volcanic origin of the Gamburtsev Subglacial Mountains, Antarctica, Geophys. Res. Lett., 35, L21303, doi:10.1029/2008GL035564.

van der Wal, W., P. L. Whitehouse, E. J.O. Schrama, Effect of GIA models with 3D composite mantle viscosity on GRACE mass balance estimates for Antarctica, Earth Planet. Sci. Lett., 414, 134-143, 2015.

Wannamaker, P., Hill, G., Stodt, J., Maris, V., Ogawa, Y., Selway, K., et al. (2017). Uplift of the central transantarctic mountains. Nature Communications, 8(1), 1588. https://doi.org/10.1038/s41467-017-01577-2

Watson, T., A. Nyblade, D. A. Wiens, S. Anandakrishnan, M. Benoit, P. J. Shore, D. Voigt, and J. VanDecar (2006), P and S velocity structure of the upper mantle beneath the Transantarctic Mountains, East Antarctic craton, and Ross Sea from travel time tomography, Geochem. Geophys. Geosyst., 7, Q07005, doi:10.1029/2005GC001238.

Weaver, S. D., Storey, B. C., Pankhurst, R. J., Mukasa, S. B., DiVenere, V. J., & Bradshaw, J. D. (1994). Antarctica-New Zealand rifting and Marie Byrd Land lithospheric magmatism linked to ridge subduction and mantle plume activity. Geology, 22(9), 811–814. https://doi.org/10.1130/0091-7613(1994)022<0811:ANZRAM>2.3.CO;2

Whitehouse, P. L., N. Gomez, M. A. King, and D. A. Wiens, Solid Earth change and the evolution of the Antarctic Ice Sheet, *Nature Comm.*, https://doi.org/10.1038/s41467-018-08068-y, 2019.

Wobbe, F., K. Gohl, A. Chambord, and R. Sutherland (2012), Structure and breakup history of the rifted margin of West Antarctica in relation to Cretaceous separation from Zealandia and Bellingshausen plate motion, Geochem. Geophys. Geosyst., 13, Q04W12, doi:10.1029/2011GC003742.

Wobbe, F., Lindeque, A., & Gohl, K. (2014). Anomalous South Pacific lithosphere dynamics derived from new total sediment thickness estimates off the West Antarctic margin. Global and Planetary Change, 123, 139–149. https://doi.org/10.1016/j.gloplacha.2014.09.006

White-Gaynor, A. L., A. A. Nyblade, R. C. Aster, D. A. Wiens, P. D. Bromirski, P. Gerstoft, R. A. Stephen, S. E. Hansen, T. Wilson, I. W. Dalziel, A. D. Huerta, J. P. Winberry, S. Anandakrishnan, Heterogeneous upper mantle structure beneath the Ross Sea Embayment and Marie Byrd Land, West Antarctica, revealed by P-wave tomography, Earth Planet. Sci. Lett., 513, 40-50, 2019.

- Wilch, T. I., W. C. McIntosh, and N. W. Dunbar, 1999, Late Quaternary volcanic activity in Marie Byrd Land: Potential ⁴⁰Ar/³⁹Ar-dated time horizons in West Antarctic ice and marine cores, Geol. Soc. Am. Bull, 111, 1563–1580.
- Will, T. M. A. Zeh, A. Gerdes, H. E. Frimmel, I. L. Millar, E. Schmädicke (2009), Palaeoproterozoic to Palaeozoic magmatic and metamorphic events in the Shackleton Range, East Antarctica: Constraints from zircon andmonazite dating, and implications for the amalgamation of Gondwana, *Precambrian Research*, 182, 25-45.
- Wilson, D. S., and B. P. Luyendyk (2009), West Antarctic paleotopography estimated at the Eocene-Oligocene climate transition, Geophys. Res. Lett., 36, L16302, doi:10.1029/2009GL039297.
- Yamasaki, T., H. Miura, and Y. Nogi (2008), Numerical modelling study on the flexural uplift of the Transantarctic Mountains, Geophys. J. Int., 174, 377-390.
- Yuan, Y.O., Simons, F.J. and Tromp, J., 2016. Double-difference adjoint seismic tomography. Geophysical Journal International, 206(3), pp.1599-1618.
- Zhang, S. & Karato, S., 1995. Lattice preferred orientation of olivine aggregates deformed in simple shear, *Nature*, **375**, 774–777.
- Zhou, Z., D. A. Wiens, W. Shen, S. Hansen, R. Aster, A. Nyblade, 2019. Radial anisotropy of Antarctica from surface wave ambient noise tomography, Seism. Res. Lett., 90, 1047.
- Zhu, H., Bozdağ, E., & Tromp, J. (2015). Seismic structure of the European upper mantle based on adjoint tomography. Geophysical Journal International, 201(1), 18–52. https://doi.org/10.1093/gji/ggu492

Figure Captions

- **Fig 1.** Map of broadband seismic stations deployed in Antarctica and used in recent seismic studies. Permanent seismic stations, generally at Antarctic research stations, are shown as green boxes, and temporary seismic stations are shown as triangles. The key identifies some of the larger temporary seismic station deployments.
- **Fig 2.** Shear wave splitting results for central West Antarctica from *Accardo et al* (2014). The region shown is outlined in the green box on the inset map of Antarctica. Vector azimuths denote the average fast direction of splitting for arrivals at a given station. The length of the vector is proportional to the splitting time, with splitting time scale indicated at right. Thick red vectors represent A quality results, thin red vectors represent B quality results, and black vectors represent results assembled from other studies. Solid green arrows indicate the direction of Antarctic absolute plate motion in the hotspot reference frame. Background colour scale indicates bedrock elevation from Fretwell *et al.* 2013. Abbreviations: PIR -- Pine Island Rift; BSB -- Byrd Subglacial Basin; BST -- Bentley Subglacial Trench; EWM -- Ellsworth-Whitmore Mountains, WARS West Antarctic Rift System.
- **Fig 3.** Example of joint inversion of surface wave dispersion (SW) and P-wave receiver functions (PRF) for POLENET seismic station SWEI (Shen et al., 2018b). (a-b) Observed Rayleigh wave phase and group velocity dispersion curves (a) and P-wave receiver function waveform (b) at station SWEI. The square root of the reduced χ^2 misfit for the preferred model is given in parentheses. (c-d) Results

from the joint inversion of both surface wave and receiver function data (c) and surface wave data alone (d). Gray corridors represent the 1-dimensional seismic model emsembles, with black and red lines showing the average shear velocity (V_{SV}) and the standard deviation of the 1-D model. (e) Predicted receiver function waveform from models in (c) and (d) are shown as red and gray waveforms. Observed RF with uncertainties are shown as two thick blue lines. (f-h) Prior and posterior distributions of crustal V_{SV} (15 km, f), crustal thickness (g), and mantle V_{SV} (80 km, h). Prior distributions are shown by unfilled bars, joint inversion posterior distributions are shown in red, while the surface wave inversion posterior distribution is in blue.

- **Fig 4.** Uppermost mantle V_{SV} structure from the Bayesian Monte Carlo joint inversion of surface wave dispersion and receiver functions (Shen et al., 2018b). Maps show horizontal sections for depths of 60 km (a), 80 km (b), 120 km (c), and 160 km. Dotted lines enclose the Gamburtsev Subglacial Mountains (GSM), Transantarctic Mountains (TAMS), Ellsworth-Whitmore Mountains (EWM), and Marie Byrd Land highlands (MBL).
- **Fig 5.** Crustal thickness of Antarctica. Map is based on an inversion of seismic receiver functions and Rayleigh wave velocities by Shen et al (2018b) in West and central Antarctica, and on GOCE satellite gravity constraints over the entire continent (Pappa et al., 2019a). The crustal thickness map based on gravity was corrected for a systematic crustal thickness offset with respect to the thicknesses derived from seismology. The resulting corrected gravity-based map was averaged with the seismic map in regions where the coverage overlapped. Abbreviations: AP—Antarctic Peninsula, LG—Lambert Graben, MBL—Marie Byrd Land, RE—Ross Embayment, WE—Weddell Sea Embayment, WARS West Antarctic Rift System, TAMS Transantarctic Mountains, GSM Gamburtsev Subglacial Mountains, EWM Ellsworth-Whitmore Mountains.
- **Fig 6.** Tomographic images of the shear wave velocity structure of seismic model ANT-20 at 75-, 150-, 250-, and 350-km depth from *Lloyd et al* (2020). Bathymetry and bedrock topography contours for 1,000 m (thin white line) and –500 m (thin brown line), as well as –2,500 m (thin dark gray line) in the oceans are also shown (Fretwell et al., 2013). Abbreviations: AT—Adare Trough, AS—Amundsen Sea, AP—Antarctic Peninsula, BI—Balleny Islands, BS—Bellingshausen Sea, LG—Lambert Graben, LHB—Lützow-Holm Bay, MTJ— Macquarie Triple Junction, MBL—Marie Byrd Land, RE—Ross Embayment, RI—Ross Island, SSR—South Scotia Ridge, TI—Thurston Island, WE—Weddell Embayment.
- **Fig 7.** Lithospheric thickness of East Antarctica based on the ANT-20 seismic model (Lloyd et al., 2020). Lithospheric thickness was calculated from velocity profiles assuming the bottom of the lithosphere is located at the depth of the maximum negative velocity gradient above the low velocity zone (Van der Lee, 2002). Geographic labels are the same as in Fig. 5.
- Fig 8. Average V_S in the uppermost 50 km of the mantle beneath central Antarctica, showing the absence of cold, fast mantle lithosphere beneath the Transantarctic Mountains (Shen et al., 2018a). Black lines indicate the locations of the two vertical profiles shown in fig. 9. A small open box marks the approximate location of the Mount Early and Sheridan Bluff volcanism. The Transantarctic Mountains (TAMS), the Ellsworth-Whitmore Mountains (EWM) and the Ross Embayment (RE) are labeled. Lines AA' and BB' denote the location of the cross sections shown in Fig. 9.

- **Fig 9.** Cross sections beneath the Southern Transantarctic Mountains and Whitmore Mountains along lines AA' and BB' in figure 8, from Shen et al (2018a). Panels (a) and (b) show vertical V_S , and panels (c) and (d) show the corresponding interpretation. V_S in the crust is plotted as absolute value, and V_S in the mantle is plotted as the percent perturbation relative to the averaged 1D V_S structure of the study region. Geographic features are marked by abbreviations: West Antarctic Rift System (WARS), Ross Embayment (RE); Transantarctic Mountains (TAMS); Whitmore Mountains (WM); Thiel Mountains (TM).
- **Fig 10.** Comparison of P-wave traveltime tomography (Hansen et al., 2014) with adjoint waveform tomography (Lloyd et al., 2020) results for a profile across the Amundsen Sea (AS), Marie Byrd Land (MBL), the West Antarctic Rift System (WARS), and the Whitmore Mountains (WM), along line F in Fig 11. The images show generally similar features in areas below the continent with good P-wave raypath coverage (below MBL and East Antarctica), but anomalies are missing from the P-wave model in regions with little raypath coverage, such as the Amundsen Sea coast. Both models show that slow velocity anomalies beneath the Marie Byrd Land dome continue into the lower mantle, consistent with a mantle plume origin for the topography and volcanism.
- **Fig 11.** Images of shear-wave speed structure beneath West Antarctica at 75 km depth and along profiles D, E, and F, from Lloyd et al. (2020). Horizontal and vertical slices have a shear-wave speed range of $\pm 6\%$ and $\pm 2\%$, respectively. The horizontal slice depicts broadband seismic stations, wave speed anomalies, bathymetry, topography as in Fig. 6. Abbreviations: AS Amundsen Sea, ASE Amundsen Sea Embayment, AP Antarctic Peninsula, BS Bellingshausen Sea, EWM Ellsworth-Whitmore Mountains, MBL Marie Byrd Land, TAMS Transantarctic Mountains, TI Thurston Island, WARS West Antarctic Rift System, WSE Weddell Sea Embayment, WM Whitmore Mountains

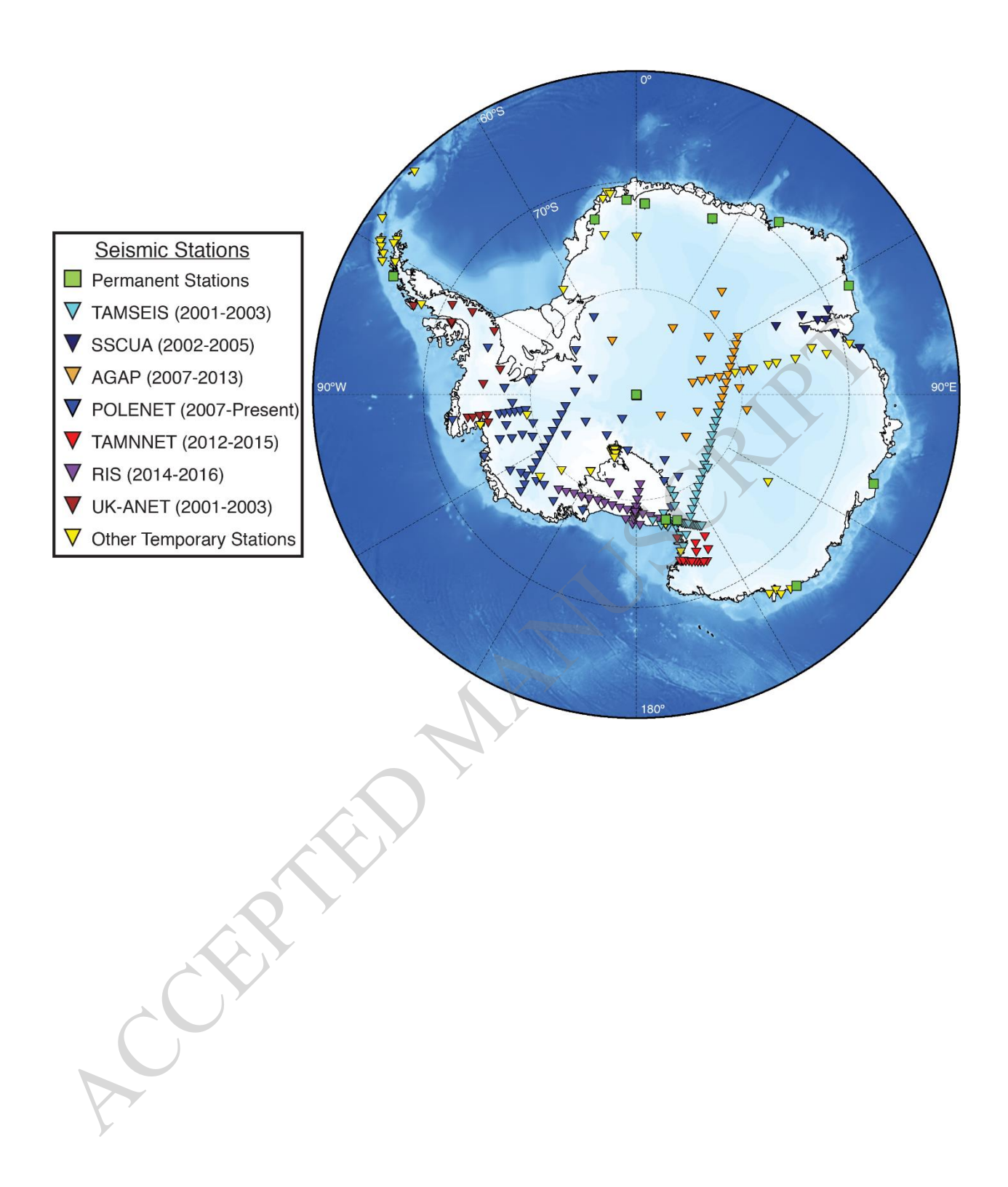


Figure 1

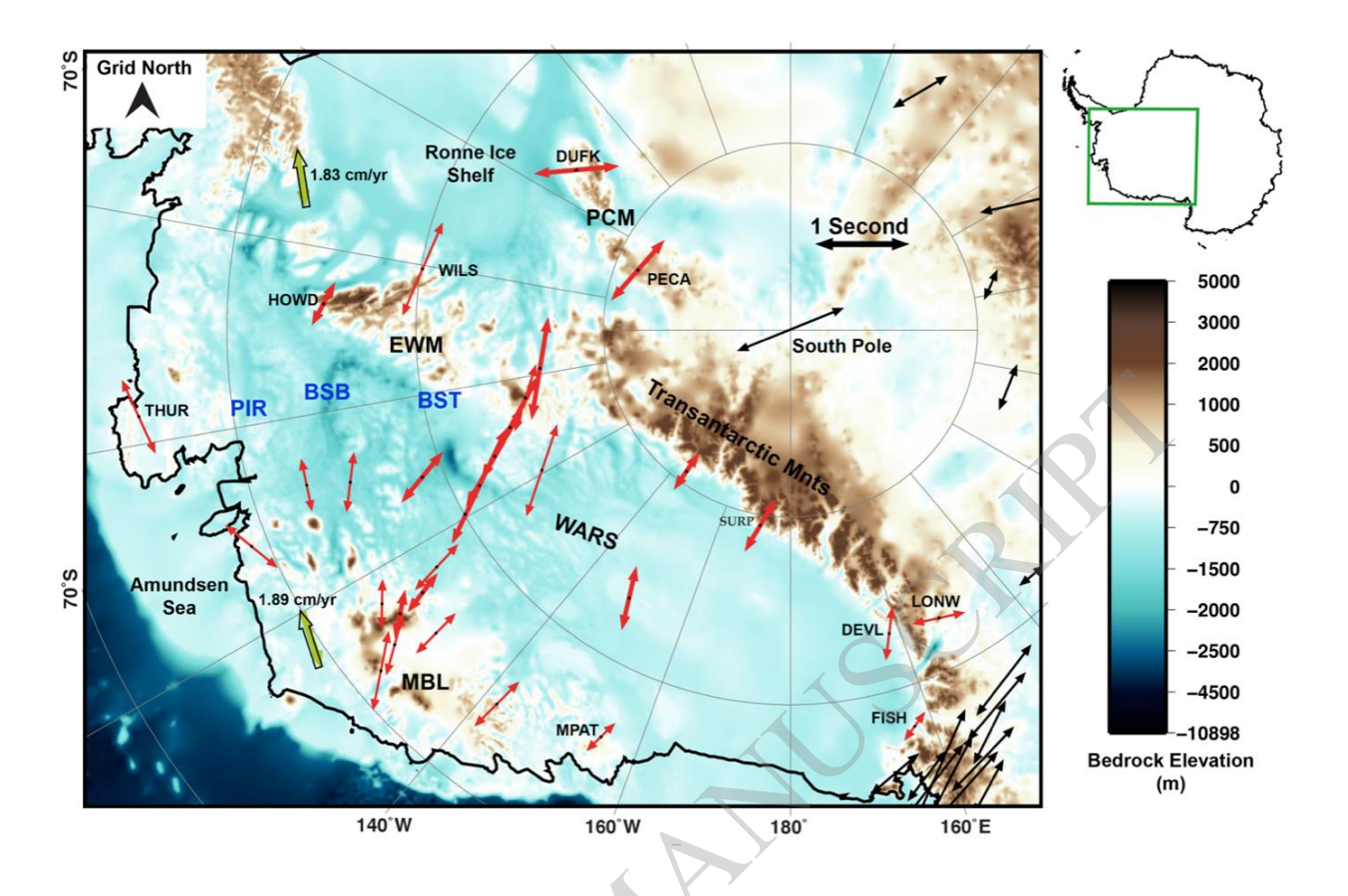


Figure 2

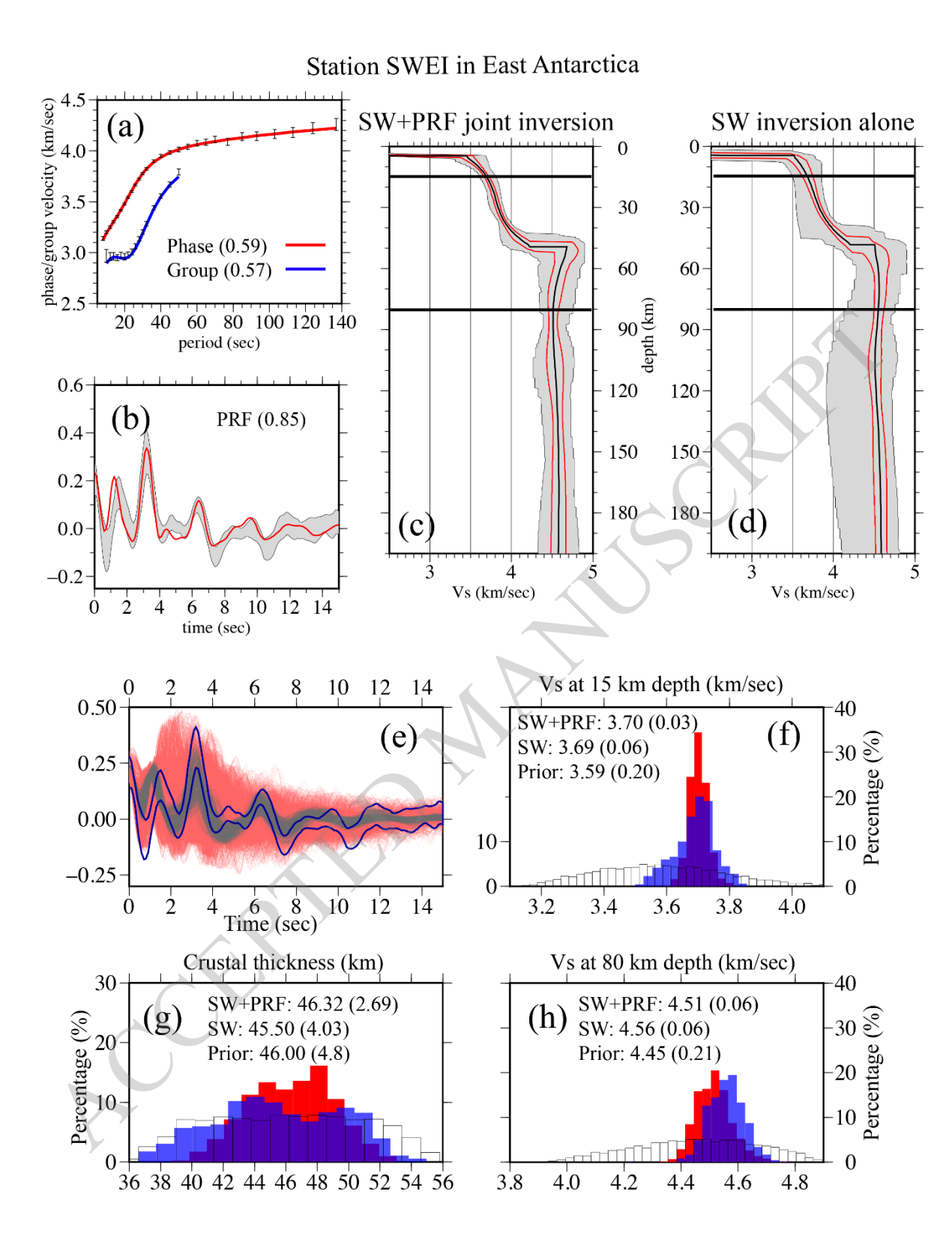


Figure 3

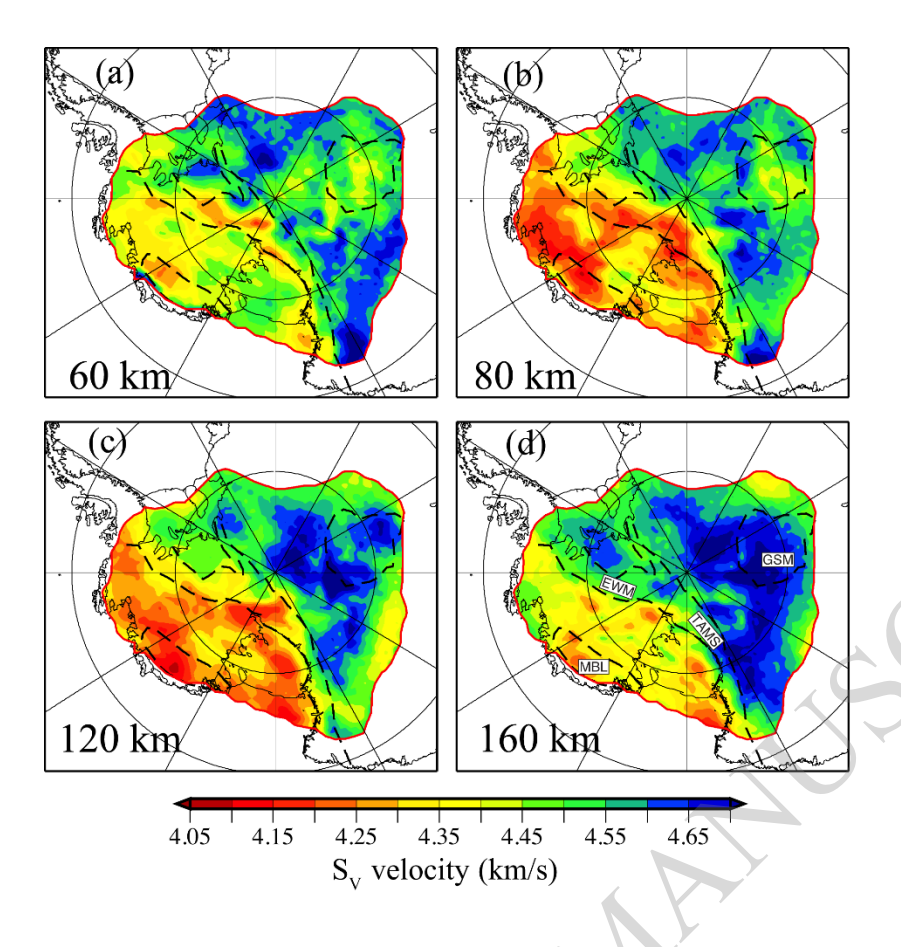


Figure 4

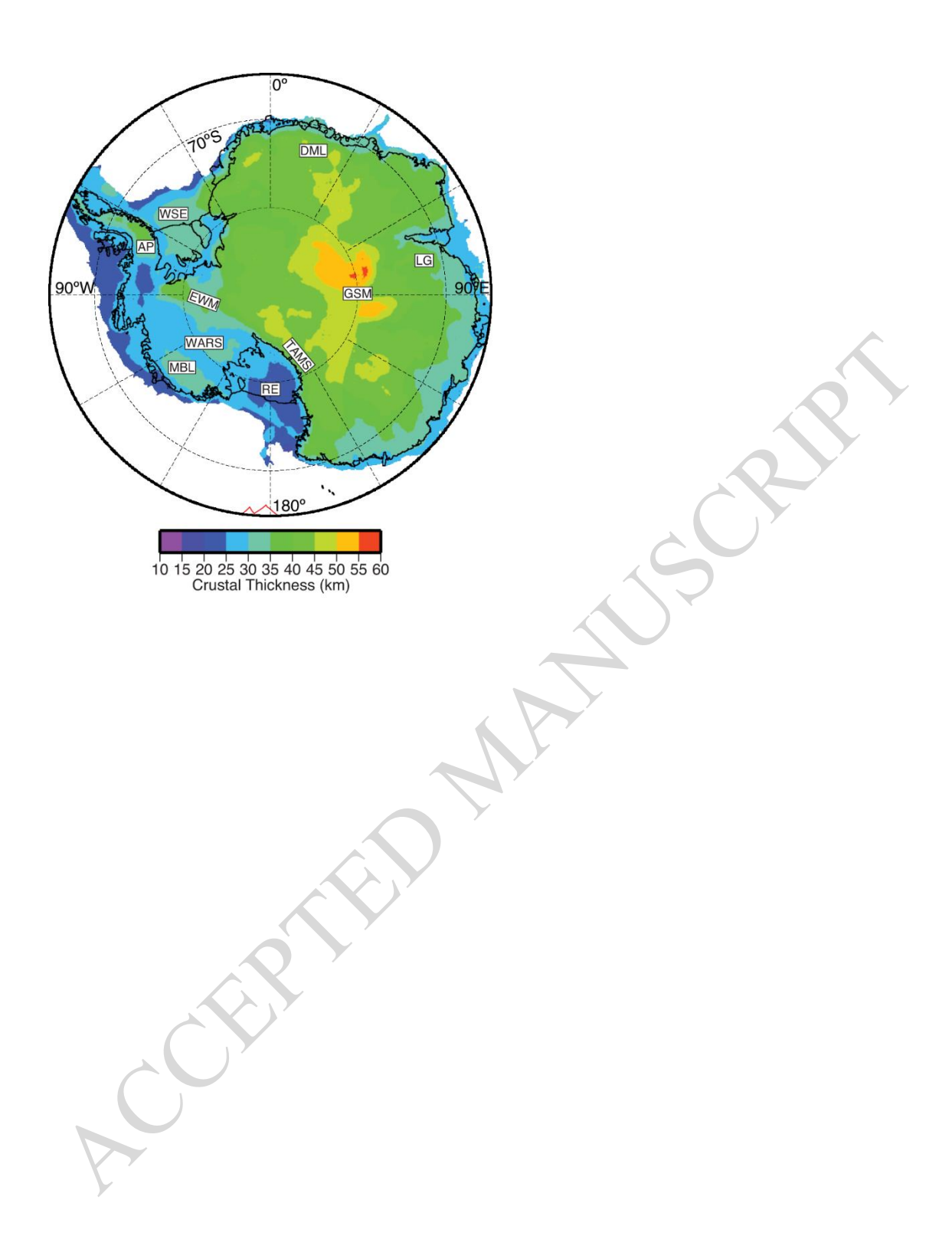


Figure 5

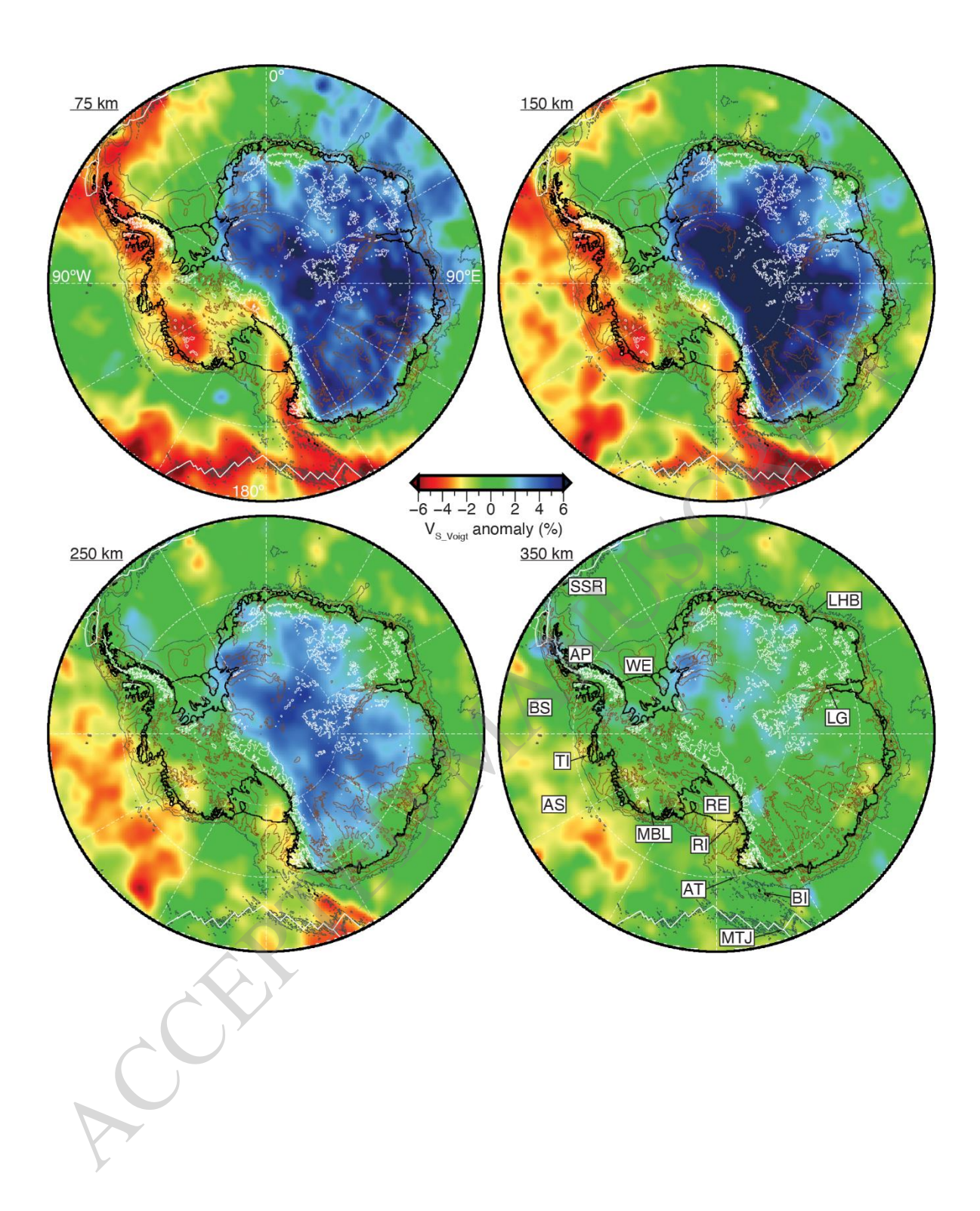


Figure 6

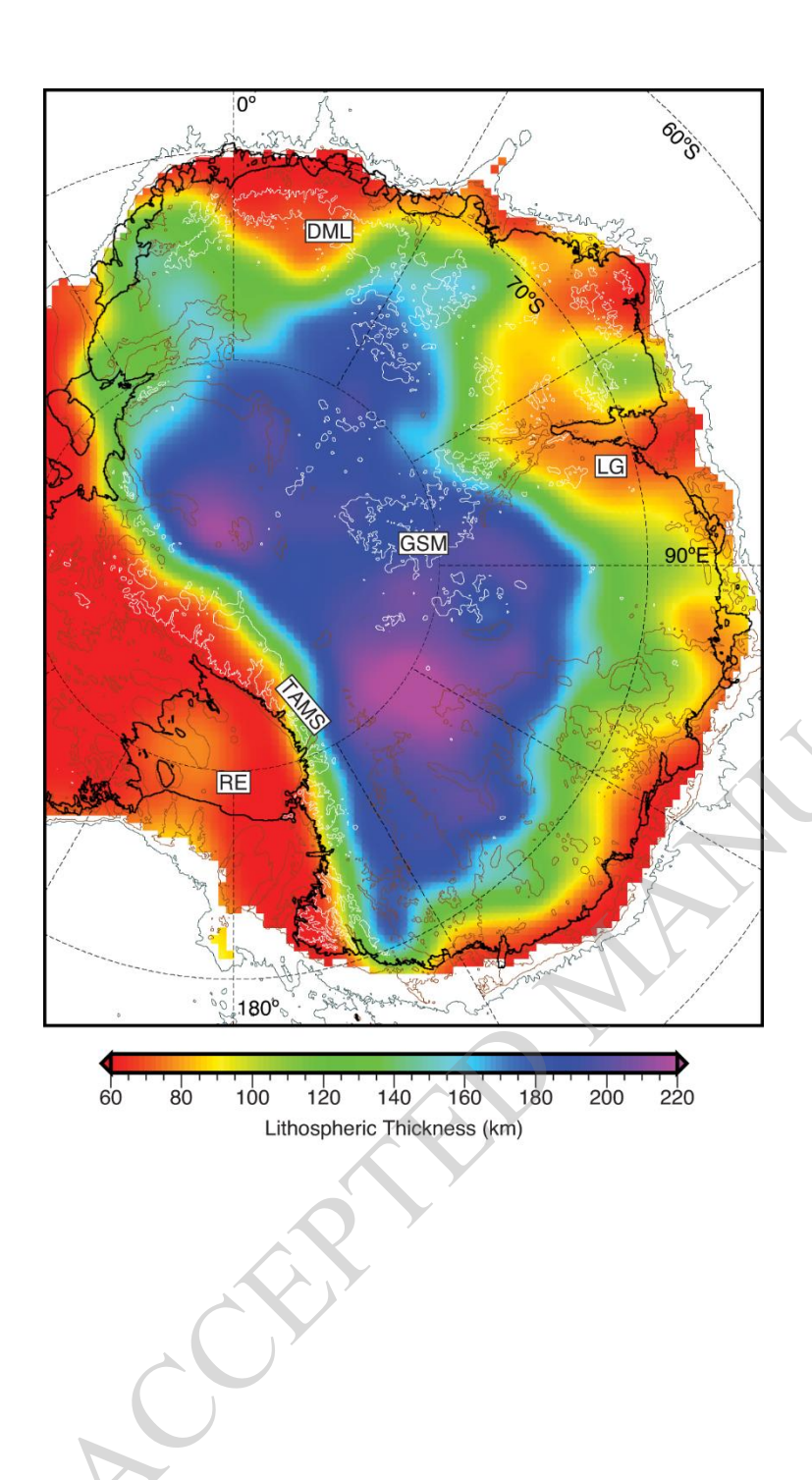


Figure 7

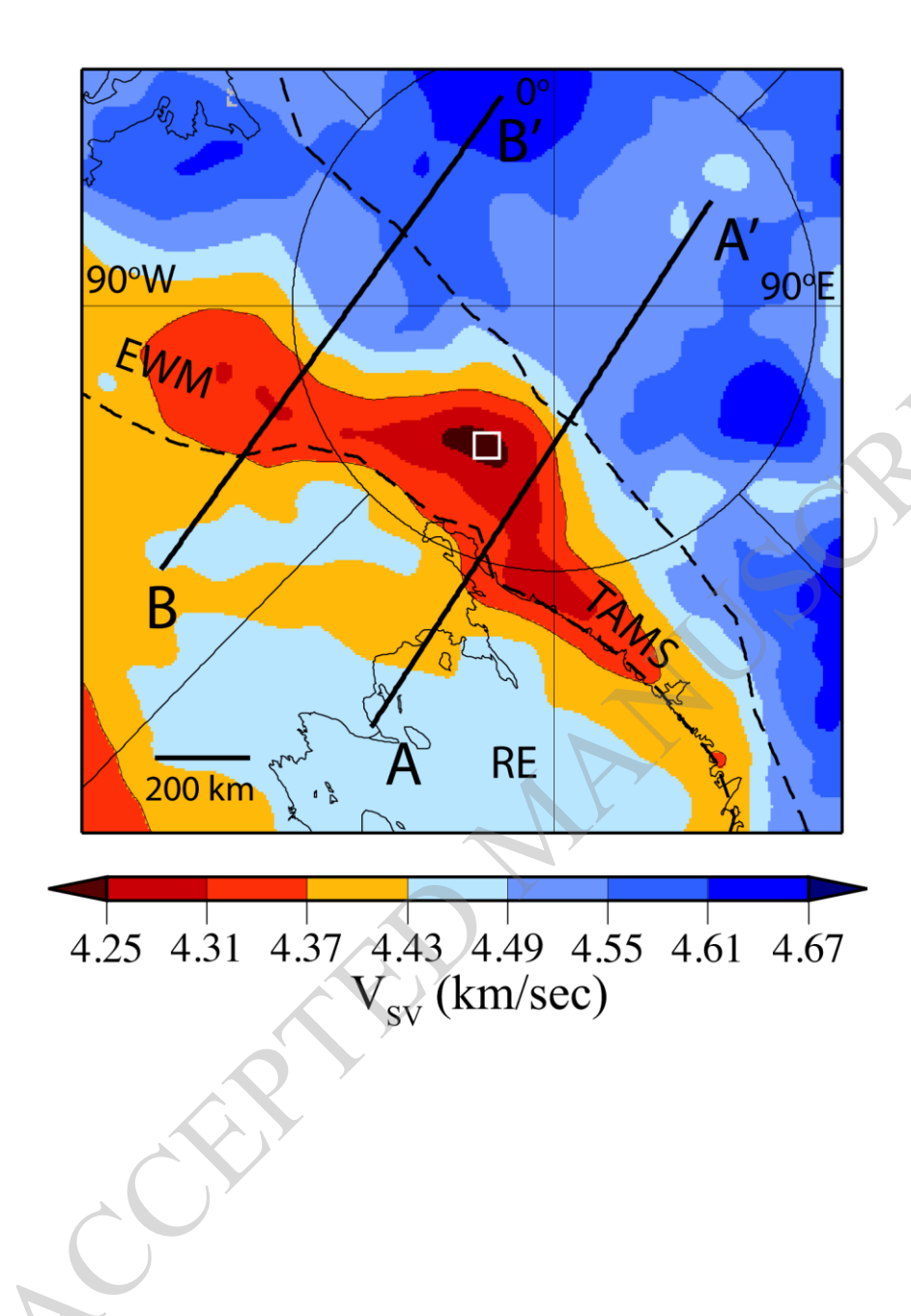


Figure 8

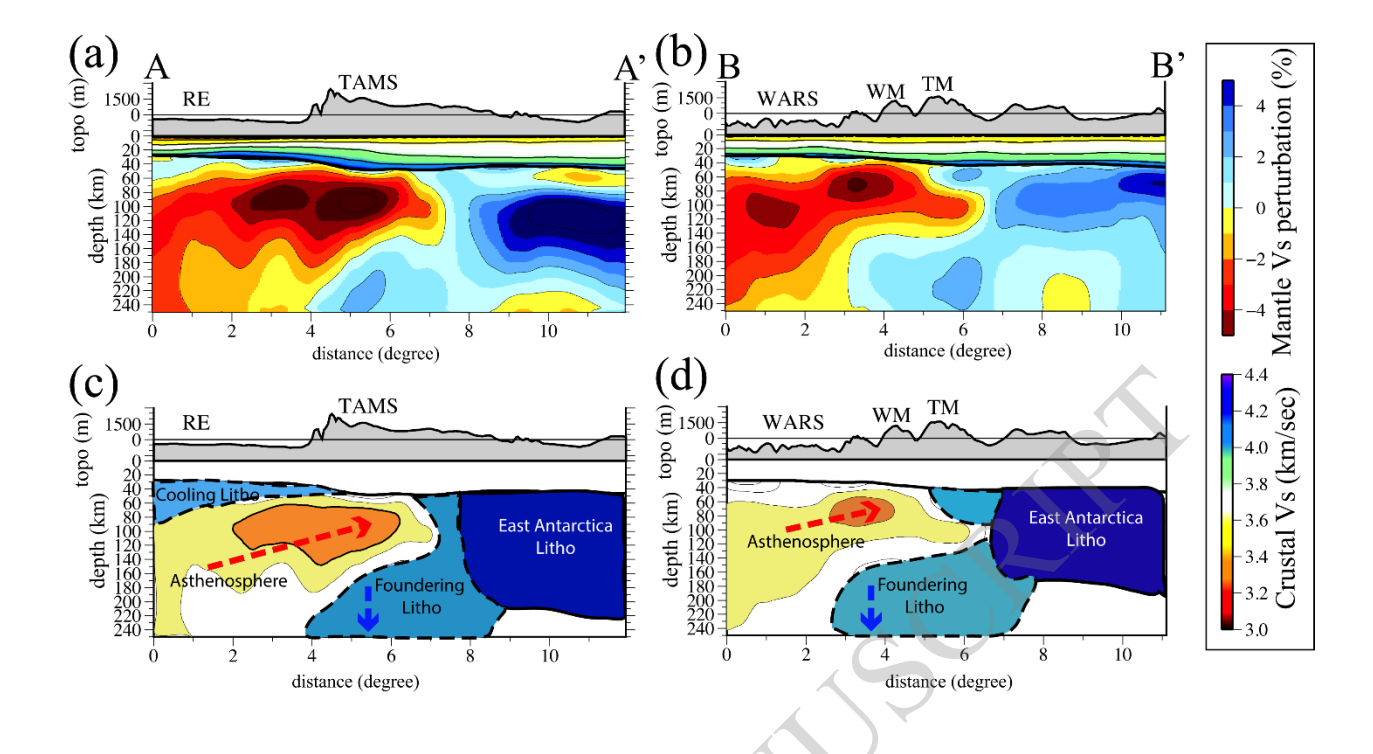


Figure 9

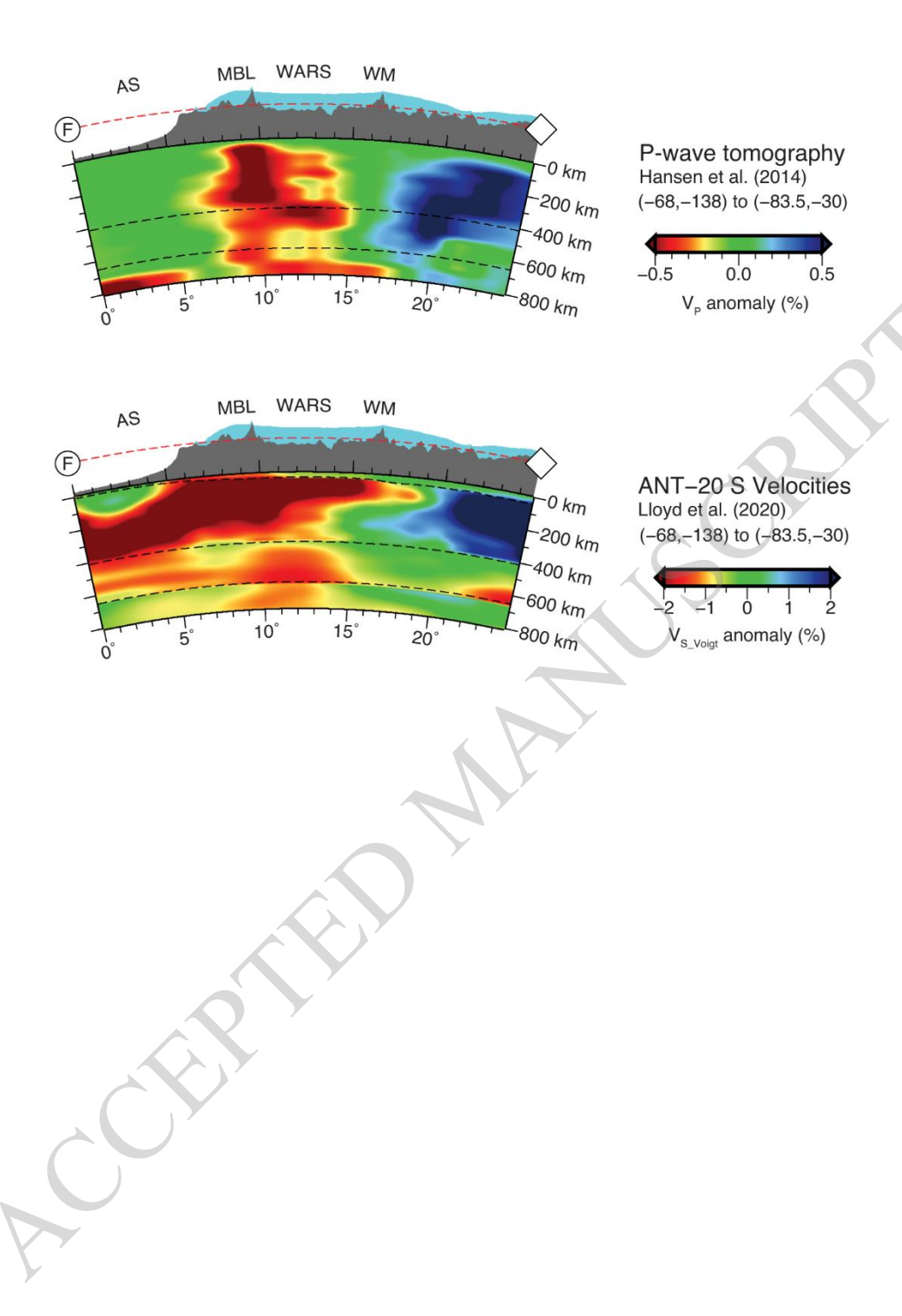


Figure 10

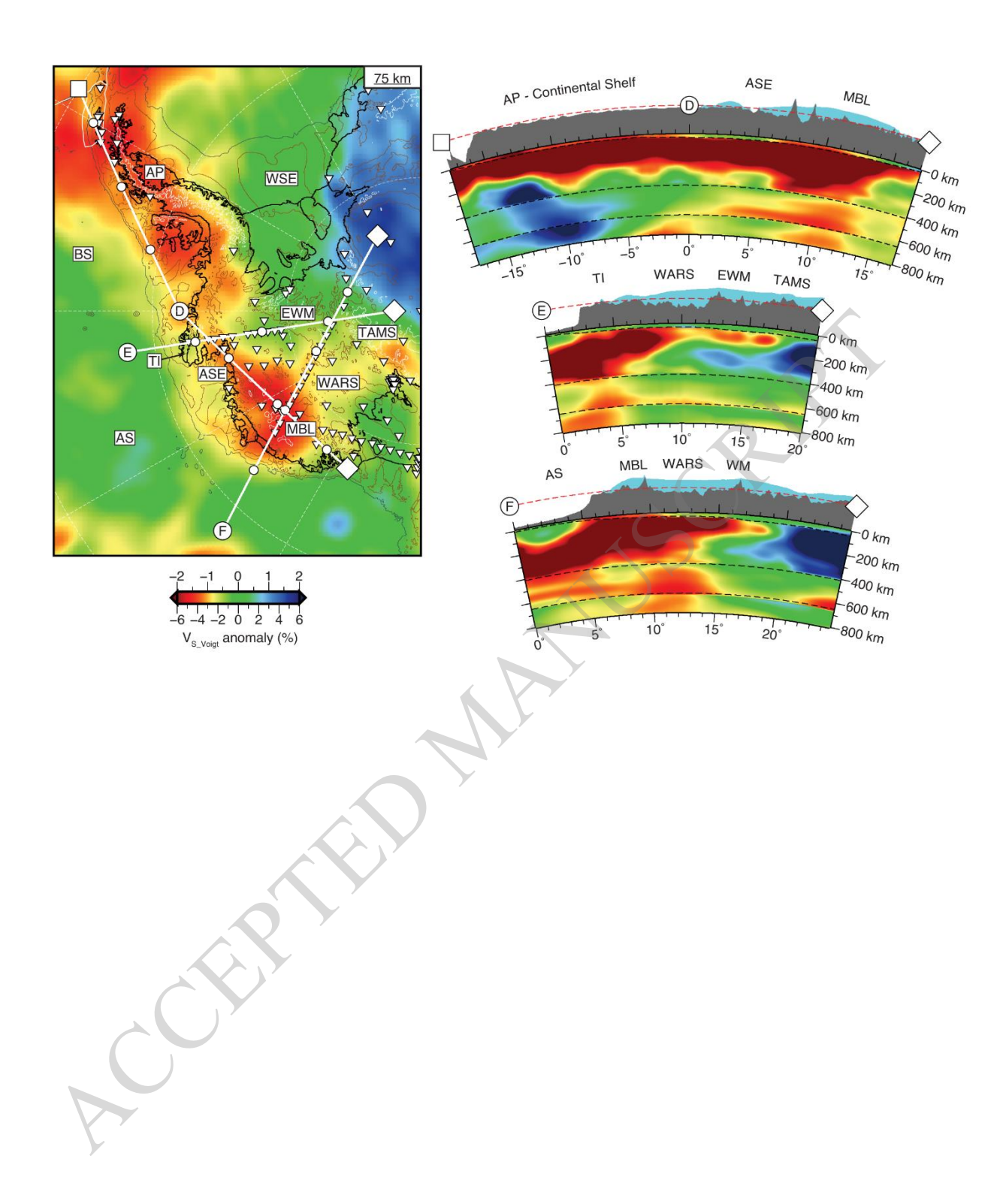


Figure 11